2012

Active combine speed control for relative positioning of a grain cart

Alex Jon Nykamp
Iowa State University

Active combine speed control for relative positioning of a grain cart

by

Alex Jon Nykamp

A thesis submitted to the graduate faculty
in partial fulfillment of the requirements for the degree of
MASTER OF SCIENCE

Major: Agricultural Engineering

Program of Study Committee:
Matthew Darr, Major Professor
Brian Steward
Steven Hoff

Iowa State University
Ames, Iowa
2012

Table of Contents

List of Figures

List of Tables

Acknowledgements

I would like to thank Deere and Company for providing the funding and equipment for this research. Thanks is given to Dr. Matt Darr for providing me with this research, as well as the valuable advice and guidance given throughout the project. I would also like to thank Dr. Steven Hoff and Dr. Brian Steward for their willingness to serve on my program of study committee.

Sincere thanks is also given to all my colleagues who assisted me in the completion of this project through support given for both development and testing. Specifically, I am grateful to Andy Jennett, John Kruckeberg, Robert McNaull, and Ben Potter for their many hours of assistance.

Deepest gratitude and thanks is also given to my loving wife, Shannon. Although this project required many long days to complete the development and testing, her continued support, encouragement, and love was steadfast and greatly appreciated.

Above all, I thank God for giving me both the ability and opportunity to complete this research.

Chapter 1. Introduction

In the past, optimizing the efficiency of crop production focused on one single machine. Today, machine manufacturer's focus has shifted to optimizing the performance of a complete field operation through coordinated machine operations.

The focus of this project was on the harvest operation, where resource usage is typically the highest. With modern grain harvest systems, combine operators often unload grain while continuing to harvest crop (unloading-on-the-go). In order to achieve this, the combine operator must coordinate machine speed and placement with the grain cart operator for accurate placement of grain into the cart. The combine operator manages on/off control of the unloading auger with in-cab controls as the well as the placement of the grain by changing the speed of the combine relative to the cart.

This project developed an autonomous machine positioning system that controlled the relative position of a combine to a grain cart during unloading-on-the-go. This was achieved by developing a control model which made small adjustments to the ground speed of the combine to achieve relative position shifts.

The control system was able to consistently achieve the desired accuracy of ±40 cm while limiting the differential engine loading due to position shifts to less than 10% of the rated engine power. In addition, the system was tuned to make position shifts at a similar rate as that of an operator during traditional operation.

Analysis was performed on the step response characteristics of the system across treatment factors of ground speed, allowable range of speed, and engine load. The results showed a statistically insignificant impact of ground speed and engine load, while range of speed did have a statistically significant impact on response time.

This result of this project was a system that allowed the combine operator to completely remove attention from the combine's relative positioning to the grain cart during a grain unloading cycle.

Chapter 2. Literature Review

2.1. Relative Position Control in Other Industries

2.1.1. Automotive: Adaptive Cruise Control

Adaptive Cruise Control (ACC) was first made commercially available in 1998 and is now available in various levels from nearly every major automotive manufacturer (Vollrath, Schleicher and Gelau 2011). ACC is an extension of the traditional cruise control system, which simplifies driving by relieving the driver of the task of maintaining constant speed. ACC further simplifies the task of driving a car because it relieves the driver of the task of continual awareness of the car's relative velocity to other vehicles.

When the car is on the open roadway, ACC performs like traditional cruise control by maintaining a constant vehicle speed set by the driver. The primary difference is that if a car with ACC approaches a slower moving vehicle it will automatically decelerate to maintain a constant time gap between the vehicles. The constant time gap is defined as the time required for the front edge of the car to reach the current location of the back edge of the vehicle ahead in the path of travel. If the deceleration due to the drivetrain and aerodynamic drag is insufficient to slow the vehicle at the rate required by ACC, the brakes will be applied to help avoid a collision, as shown in Figure 2.1 (Bauer 2003). If the slower vehicle exits the path of travel, ACC allows the traditional cruise control system to accelerate the vehicle back to the speed set point.

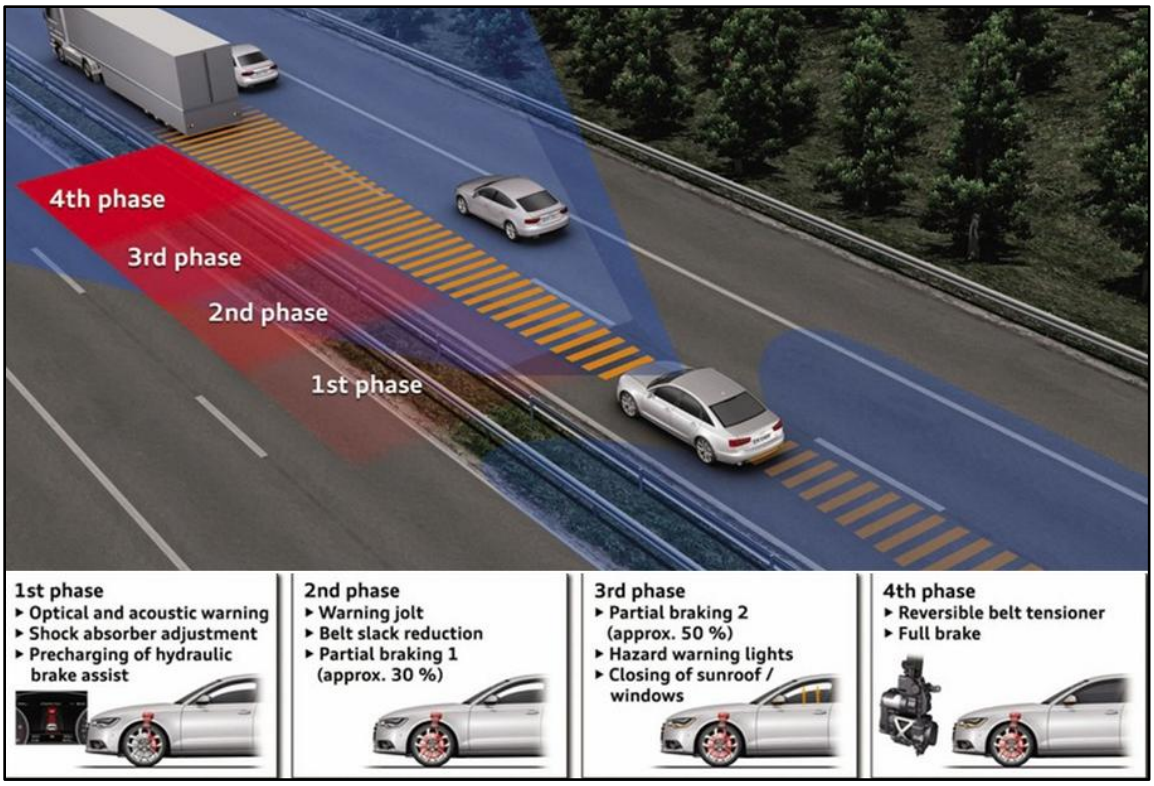

Figure 2.1: Audi Adaptive Cruise Control with Brake Assist (Photo credit: Audi)

2.1.2. Adaptive Cruise Control hardware

ACC requires only a few additional pieces of hardware to make the system fully functional. The most critical piece of hardware is that which detects the distance from other vehicles on the road. In preliminary systems, both RADAR (Radio Detection and Ranging) and SONAR (Sound Navigation and Ranging) were tested, but RADAR was found to be superior due to its performance in adverse weather conditions (fog, rain, snow, etc.). The other piece of hardware that all ACC systems have is a dedicated ACC unit. Often, the control unit is integrated into the RADAR hardware, as is the Bosch ACC system shown in Figure 2.2. (Bauer 2003)

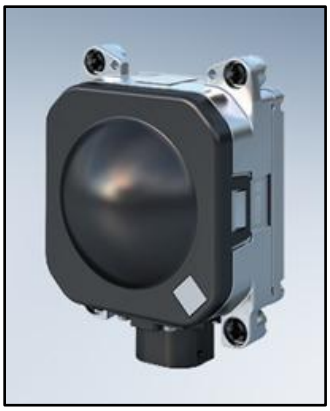

Figure 2.2 Bosch long-range RADAR sensor and ACC control unit
(Photo credit: Robert Bosch GmbH)

As the performance of ACC systems continues to improve, manufacturers have started using additional sensing technologies such as infrared, and stereo-camera based systems to obtain as much information as possible about the surrounding environment. Stereo-camera based systems have been put in place to gather information about the vehicle's position in the highway lane and detection of vehicles approaching from the rear (Onken and Schulte 2010).

In order to ensure reliable ACC system performance across changing road conditions, the Electronic Stability Program (ESP) provides ACC important sensor signals regarding the dynamic handling of the vehicle. These signals typically include information regarding yaw rate, lateral acceleration, wheel speed, and steering angle. (Bauer 2003)

The remaining piece for a fully functional ACC system is integration with the engine and transmission controller, as well as the brake controller. Typically the brakes do not have a dedicated controller, so ACC will send braking commands to the ESP, which will decide if the braking commands are safe to execute. With these integrations, the current production ACC system has been a success by achieving robust and stable control even across varying road surface co-efficient of frictions (wet, dry, or icy) and cornering conditions (Auckland, et al. 2005). The result is a system that is safe to operate and can typically provide better control than human manual operation.

2.1.3. Adaptive Cruise Control for Heavy-Duty Vehicles

ACC systems are being developed to broaden the range of ACC application, particularly in the area of heavy duty vehicles. Heavy-duty vehicles require a very different set of system parameters due to higher weight-to-power ratio, the much larger vehicle mass, as well as the amount that vehicle mass can change (up to 400% variance depending on payload). Bengea *et. al.(2006)* of Eaton Corporation has developed a control system that moved away from the typical control system architecture, which used throttle and brake signals, to a control system that used engine torque as the control signal to address the unique heavy duty vehicle parameters. Engine torque can be controlled through the torque limiting command (during positive torque) and the engine retarder (to achieve negative torque), both signals are available through the J1939 standardized Controller Area Network (CAN) bus. As with other ACC systems, this ACC system works in conjunction with the traditional cruise control system which maintains vehicle speed to a driver speed set point. The ACC system only has the capacity to limit the torque requests sent from the cruise control system. For accelerations, the traditional cruise control system is used to bring the vehicle back up to the speed set point. (Bengea, et al. 2006)

2.1.4. Adaptive Cruise Control Current Progress

A further development in the field of ACC is Cooperative Adaptive Cruise Control (CACC), which can communicate with other vehicles traveling in close proximity. It is expected that CACC can enhance and help promote stable flow in heavy traffic environments by eliminating driving behavior that varies on an individual level. However, a production system of CACC is several years away. Significant developmental work is still needed to develop the technologies to be used, and gain adequate knowledge to properly design a control model for optimum traffic flow. (Pueboobpaphan and Arem 2010)

2.1.5. Mining: Autonomous Mining Vehicles

In the mining industry, autonomous systems have been developed to increase employee safety and mining efficiency. The dangerous work of mining can be eliminated by implementing these autonomous systems, which allow work vehicles to be monitored from a remote location, away from the hazardous situations a mine presents. Also, many mines deal

with a continual labor shortage due to the remote locations of the mines. This problem can be partially fixed with these autonomous systems which no longer require employees to perform monotonous tasks, but instead allow one employee to monitor the work of multiple machines.

The Caterpillar MineStar system provides technology for remote control, semi-autonomous, and autonomous control systems. In the completely integrated solutions, the machines are directed where to go and what to do, but an on-board intelligence system decides how to navigate and accomplish the task.

For underground mining, the Caterpillar Minestar system is a semi-autonomous system that allows a single operator to control and monitor multiple wheel loaders. During the typical load-haul-dump cycle the operator completes the load and dump tasks from a remote control station. During the haul portion, the machine is controlled autonomously to drive from the loading location to dumping location. Not only does this technology provide mines with improved worker safety, but also improved equipment use and efficiency as the equipment does not stop for shift changes or evacuation times needed following a blast (Caterpillar 2011).

For open pit mining the Caterpillar Minestar system provides a completely autonomous solution that allows trucks to haul without an operator. In order to avoid collisions with other vehicles and objects, the Minestar Detect system works to recognize possible hazards in the vehicles path of travel through several means. For short range detection the vehicle is outfitted with radar sensors to notify the system when an object is detected. For long range detection the trucks use the Global Navigation Satellite System (GNSS) (currently a combination of the United States' GPS system and the Russian GLONASS system) for navigation and to locate other trucks and mine assets. For all non-permanent mine equipment (service trucks, portable equipment) individual electronic tags are attached allowing both the autonomous system and remote operators to recognize the location of all vehicles in the mine. (Engineering and Mining Journal 2011)

Figure 2.3 A Cat Mining Truck using Minestar software and GNSS position information to operator autonomously. (Photo credit: Caterpillar)

Kotmastu first announced their Autonomous Haulage System (AHS) early in 2008, and has since deployed the system to two open-pit mines, one in Chile, the other in Australia. Both mines were located in very remote locations where securing sufficient manpower was a difficult task. For the operation located in Australia, all trucks are controlled via a remote operations center over 600 miles away in Perth, where labor resources are much more abundant.

The Kotmatsu AHS system provides fleet management for all vehicles in the mine, and position control for dump trucks. These dump trucks are equipped with GNSS receivers to receive position data, obstacle detection systems, and a wireless network which allows machines to communicate with each other. When the trucks near the loading spot, they are automatically guided to the bucket of the GNSS equipped excavator or wheel loader. The system is still labeled as proprietary, and is not commercially available for purchase by mining companies (Komatsu 2011).

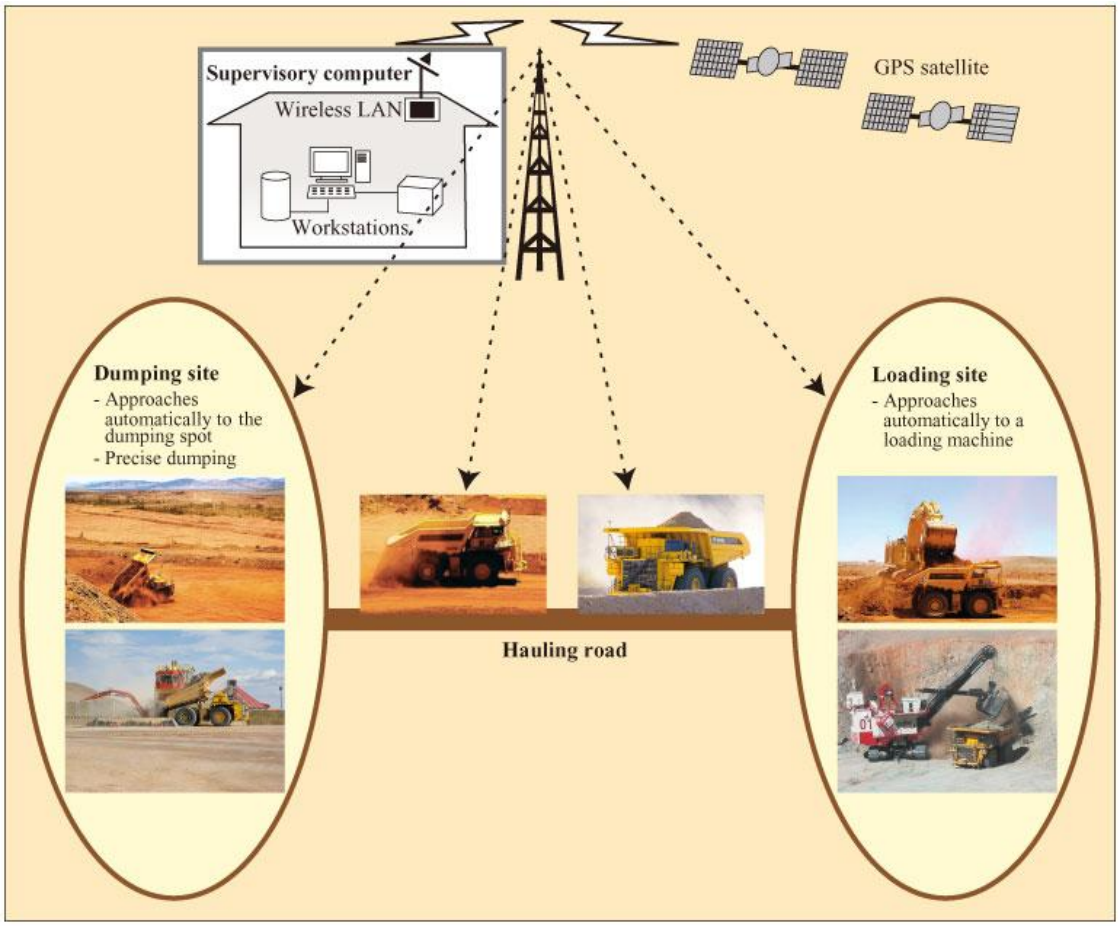

Figure 2.4: Overview of the Komatsu Autonomous Haulage System (Photo credit: Komatsu)

2.2. Combine Speed Control Systems to Optimize Crop Flow

Combine speed control systems are not a new area of development for the harvesting industry. Starting in the 1970's and moving forward, several manufacturers have put development resources into combine speed control systems used to maintain optimal crop flow through the machine.

2.2.1. Early Combine Speed Control Systems

In 1971, two patents were filed for a control system to automatically control combine ground speed by inventors working for Massey Ferguson. E. L. Elfes patented a system which used vacuum tubes to amplify grain loss signals. (Stone, Benneweis and Bergeijk 2008). These grain loss signals were transmitted to a controller that converted the signal to

an output proportional to the grain impacting the sensor. This output was sent to a solenoid valve that controlled a hydraulically operated variable speed drive. (Elfes 1971) Also in 1971, Franz Herbsthofer patented a similar system which used grain loss signals as the control system input. In this case, the ground speed control was achieved using a solenoid which actuated the control for a variable V-belt drive, attached to the drive wheels. This system used an additional solenoid to switch a two-stage governor on the engine to increase the speed of the threshing drum assembly (Herbsthofer 1971).

In 1978 R. G. Fardal of International Harvester patented a system which used an analog circuit to monitor separator and feed load sensors in addition to the grain loss monitors. These analog signals were then processed by a machine speed controller which determined a change in vehicle speed to improve threshing quality. The combine drive wheels were propelled with a hydrostatic transmission which had a control element linked to a hydraulic cylinder driven by a signal from the feedrate control system. (Fardal and Rickerd 1978)

Although neither system received strong industry acceptance, these early steps by manufacturers such as Massey Ferguson and International Harvester paved the way for future autonomy in combine speed control.

2.2.2. Modern Combine Speed Control Systems

In the current market, there are combine speed control systems available from two manufacturers. These systems have nearly the identical purpose that inventors at Massey Ferguson and International Harvester had 40 years prior; automatically determine and maintain optimal crop flow through the machine.

John Deere's Harvest Smart system was the first to the market as an optional feature on the 70 series combines, model year 2008 (John Deere 2007). The system uses separator load, grain loss sensors, and engine load to automatically determine the desired changes in ground speed. These signals are all available on the machine's CAN bus, and are processed by the Harvest Smart Controller, which then outputs a desired ground speed to the ProDrive transmission controller. (Taylor, Hobby and Schrock 2005)

New Holland's IntelliCruise system was released as an optional feature on their 8000 and 9000 series combines, model year 2010. New Holland's system operates in a very similar

manner to the John Deere Harvest Smart system by monitoring several machine load and grain quality indicators to determine an optimum speed. The New Holland system claims to have an improved response time to changing crop conditions by also monitoring the power demand of the header drive. (New Holland 2011)

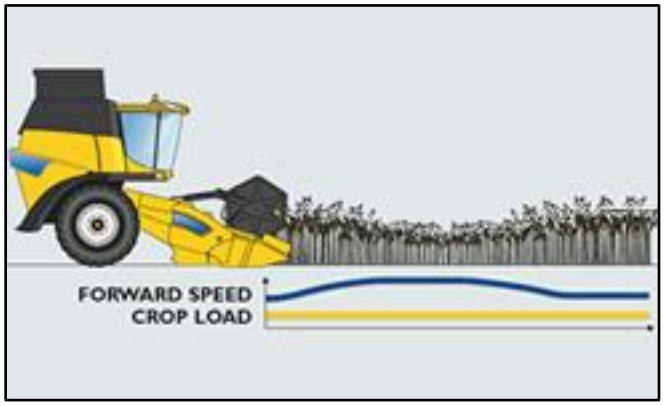

Figure 2.5: New Holland's IntelliCruise system automatically matches forward speed to crop load. (Photo credit: CNH)

2.3. Coordinated Machine Positioning in Agriculture

2.3.1. Semi-Autonomous Tractor/Grain Cart Systems

In the last two years, there has been significant development for coordinated positioning of machinery in the agricultural industry, specifically relating to the positioning of a grain cart relative to a combine. These systems have been developed to aid operators when unloading-on-the-go. Recently, both CNH and John Deere have announced systems with this capability (systems marketed as Case IH Vehicle-to-Vehicle (V2V) and John Deere Machine Sync). In these systems the combine is a central master, and it can cycle control between multiple tractor/grain cart slaves, through an in-field wireless network and vehicle GPS information. Prior to engagement, the slave must enter an operational zone near the combine, and signal that the tractor/grain cart is ready to receive position commands through a user input. When operating these machines in synchronization, the combine operator continues harvesting grain as normal, while the tractor autonomously steers and adjusts speed to position itself in a desired location to the combine. As the grain cart fills, either the combine or tractor operator is allowed to nudge their position in order to achieve an optimal cart fill. Although both systems still require an operator to remain in the cab of the tractor to engage the system upon approaching a desired master, the tractor operator is no longer

responsible for any machine control once the system is engaged. (CNH North America 2010) (Deere & Company 2011)

Figure 2.6: Case IH V2V system overview (Photo Credit: CNH)

2.3.2. Fully Autonomous Tractor/Grain Cart Systems

In order to further automate grain unloading operations Kinze Manufacturing Inc. and Jaybridge Robotics are working to develop a solution for grain unloading that will position the tractor/ grain cart in a desired position relative to the combine, without the need of an operator in the tractor cab. The system uses a set of sensors to ensure that the tractor does not run into permanent obstacles or other field equipment. The object detection sensors used by the system have just recently become cost-effective because of their large adaptation in the automotive industry for ACC systems. Although Kinze and Jaybridge have announced the system and demonstrated its functionality, no production date for the system has been set. (Berry, 2011).

Figure 2.7: Kinze/Jaybridge system demonstration of completely autonomous tractor control (Photo credit: Kinze Manufacturing)

2.4. Conclusion

In the past decade, great strides have been taken towards vehicle autonomy. In the automotive industry production relative position control systems that are robust and reliable are now available to customers. The ACC market continues to grow to more automotive models as further system improvements are made and the system price decreases due to increased volumes and decreasing sensor prices. For this project specifically, the approach to a heavy-duty ACC system was of interest. The high weight-to-power ratio is similar to that of modern farm equipment and the control system developed by Bengea *et. al. (2006)*of Eaton Corporation indicated the importance of understanding engine power requirements during relative vehicle positioning.

In the mining industry, the mines adapting the autonomous systems are able to see a safer working environment, increased mine efficiency, and less labor supply problems.

In agriculture too, great strides have been made. However, the industry has yet to provide a relative position control system that is open to the public. For the systems discussed in sections 2.3.1 and 2.3.2 there are concerns about the complexity, reliability and price of systems that require additional hardware on each field vehicle to create the complete in-field wireless network. Although Case IH and John Deere have both announced systems that achieve this functionality, a final, market-ready solution has yet to be provided to customers.

Chapter 3. Objectives

With modern grain harvest systems, combine operators' often unload grain while continuing to harvest crop. In order to achieve this, the combine operator must operate equipment in synchronization with the cart operator for accurate placement of grain into a cart. The combine operator manages on/off control of the unloading auger with in-cab controls as the well as the placement of the grain by changing the speed of the combine relative to the cart. This system demands a high level of operator attention and often distracts from the grain harvest itself. The result is a process operating at less than maximum efficiency and operator fatigue.

The long-term goal of the research project is to enhance the efficiency of agricultural machine systems. The specific goal is to develop an active combine speed control system which will automatically control the relative position of the combine to a grain cart. This will be achieved through vehicle response analysis, controller development, and field testing. Three specific objectives have been defined to fulfill the requirements of this project:

Objective 1: Develop a method for combine speed control and quantify ability to control relative position via combine speed.

A safe and reliable means to control the combine speed will be developed and data will be collected and analyzed to determine machine power requirements for achieving changes in ground speed and relative position. Upon completing analysis of the data, the ability to control the combine speed as a means to achieve a desired relative cart position will be determined. Ability to control will be defined using the metrics of machine response times, power requirements, and accuracy of machine placement relative to a cart.

Objective 2: Develop a control strategy architecture for active combine speed control.

Using the knowledge from the preliminary study, a control strategy will be developed to minimize the relative position error, while also limiting the power requirements to propel the machine. This control strategy will be implemented using reliable machine speed control techniques.

Objective 3: Validate system performance under normal field disturbances

Upon completion of control system design and installation, the system will be validated and fully tested in typical field conditions. In each of these tests, relative position

error, and system power requirements will be monitored and used to quantify the effectiveness of the control system.

This research is innovative because no manufacturer to date provides a relative positioning system for combines. When complete, this project should reduce the amount of operator attention to grain unloading, boost machine productivity by optimizing the grain unloading process, and improve the accuracy of grain placement.

Chapter 4. Combine Speed Control Development

4.1. Introduction

To meet the objectives described in chapter 3, a method had to be developed to control a relative position to a grain cart via combine speed. This chapter will address parts of both objective 1 and 2, which involved developing a safe and reliable means to control the combine ground speed from a relative position control model.

Successful objective completion will involve consistent speed control on a software and hardware platform that is suitable for the development of a relative position control model.

4.2. Background

For the last several decades, the drive train transmission of combines for all major agricultural manufacturers has been a hydrostatic drive system. This transmission type has been selected because of the infinitely variable drive ratios that allow machine operators to make smooth and precise speed adjustments to account for changing crop and field conditions. This transmission is ideal for a simple speed control system as it allows for large range of speed without having to switch gears or engine throttle levels. The operator makes these adjustments by controlling the position of a lever located in the combine cab. This lever is typically referred to as the hydro handle and it controls the desired speed of the combine by adjusting the angle of the swash plate in the hydraulic motor used for machine propulsion, known as a hydrostatic transmission.

On combines today, two methods are used to link the hydro handle to the swash plate on the hydrostatic transmission. The first is propel-by-cable and is the method used on the majority of combines. With this method, the hydro handle is physically linked to the swash plate by a cable. The second method is a system recently adopted by combine manufacturers that is part of a larger trend taking place in many industries to move away from traditional mechanical control, to electronic control, known as “x-by-wire”. For the discussions following, x-by-wire used for combine speed control will be referred to as propel-by-wire. On these machines, a rotary potentiometer is attached to the hydro handle (Figure 4.1) and outputs an analog voltage proportional to the position of the hydro handle. This analog signal

is provided as an input to an electronic control unit (ECU). This ECU interprets the analog voltage and outputs commands to an actuator controlling the position of the swash plate.

Figure 4.1: Hydro Handle setup for propel-by-wire

All model development was done on a John Deere 9870 combine with a factory installed propel-by-wire hydrostat control system. To control the speed of this machine, the wiring harness that connected the rotary potentiometer to the machine controller was tied into a custom harness to allow control of the analog signal sent to the machine controller. In all the control systems designed, the system operated in two discrete states depending on the position of a system enable switch. If the system was disabled, the output of the control model sent to the machine controller was identical to the input from the hydro handle rotary potentiometer. When the system was enabled the control system would output an altered analog signal to the machine controller to adjust ground speed. By using this means of control, the only physical modification made on the machine was the installation of a modified wiring harness that allowed for control from the developed combine speed controller. In the case of a hardware or software failure, an emergency stop allowed this harness to be bypassed by the factory harnessing.

Before beginning the control development it was important to identify the magnitude and accuracy of the position shifts required in a typical grain unloading event. Although the metrics set were subjective, typical harvest situations and conditions were examined to

determine these metrics. It was important to define these metric early in the project to guide control model development. First, the magnitude of the relative position changes was examined. Initially, it was attempted to establish the magnitude based on the size of a typical grain cart, but it is difficult to determine the size of a typical grain cart due to the variety of equipment sizes used by farmers today. For example, one of the leading grain handling equipment manufacturers (Brent by Unverferth Manufacturing Company) currently produces grain carts ranging from 550 bu. to 2000 bu. (Figure 4.2), which have fillable lengths of 3.82 m and 9.75 m, respectively (Brent Equipment 2012).

Figure 4.2: Brent 2000 bu. grain cart with a fillable length of 9.75 m (Photo credit: The Mitchell Farm)

With this wide range of lengths it was decided that magnitude of the relative position shift should not be grain cart specific, but rather based on a typical relative position shift that an operator would make to shift from a full section of the cart to a section that is less full. It was estimated that for the smallest cart (3.82 m) an operator would only need to make one major relative position shift during the unload cycle, while for the largest cart an operator might need three major relative position shifts. Assuming a non-fillable area near each edge, a standard relative position shift of 3.0 m was set.

The speed at which the relative position shift needed to take place was determined by examining how fast a shift would need to take place in order to avoid a spill due to overfilling. It was estimated after filling the first fill location, no more than 10% of the volume (50 bu. for the smallest cart) should be added to the cart prior to reaching the desired location. With the highest unloading rates around 3.5 bu./s, the maximum time for a major

relative position shift was rounded to 14 seconds. Therefore, the following performance metric was set:

- The active combine speed control system will complete a 3m relative position shift in 14 seconds or less.

To determine the required accuracy of the control system, the width of the stream of grain exiting the unloading auger was examined. It was estimated that the width of this grain stream was 40 cm, and that a sufficient accuracy of the control system would be the width of the grain stream. The following metric was established:

- The active combine speed control system will be able to achieve a relative position accuracy of ±40cm.

In addition a metric was developed to limit the amount of impact the active combine speed control system could have on engine load. From machine harvest data it was known that in a typical grain harvest situation the average engine load ranges between 70% and 90%. Therefore, if the speed control model induces increases in engine load of greater than 10% there would be a high risk of overloading the engine and crop separator. As a result the following metric was defined:

- The active combine speed control system will complete relative positioning without causing a differential engine load greater than 10% of the rated engine power.

4.3. Methods and Materials

4.3.1. Control Design with the Measurement Computing USB-1408FS

The model development for this system was done in MATLAB Simulink. The Simulink model offered several advantages for the model development and editing. Simulink uses model based software development and allows for accelerated model development with the use of standardized block libraries and a more visual model layout. The use of block libraries greatly decreases the amount of time spent developing a model by allowing the developer to focus on model structure and functionality, rather than individual lines of code. Simulink also allows for model development in a hierarchical design which is very useful for model organization as models grow larger and more complex (Figure 4.3 shows the inputs

block of the preliminary active speed control model). The Simulink model can run on any PC with the required software licensing.

Simulink also offered the ability to interface directly with common logging and control hardware components. In the lower portion of Figure 4.3 analog, digital, and CAN input blocks are used to directly input signals into the control model.

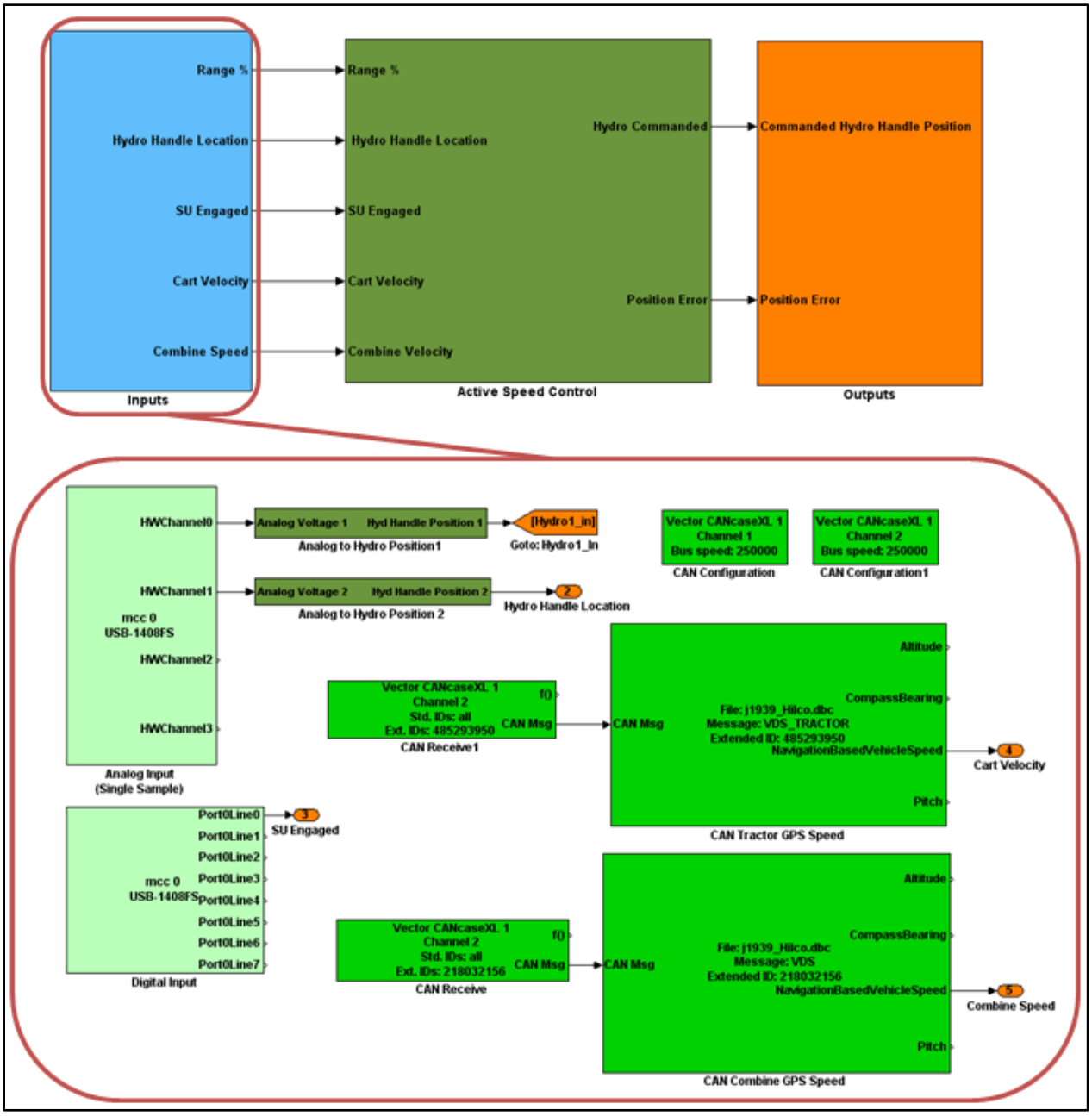

Figure 4.3: Simulink hierarchical model design of the 'Inputs' block

The controlled analog signal was output from a Simulink model that resided on a laptop computer and interfaced with a Measurement Computing USB-1408FS. The USB-1408FS provided 16 channels of digital I/O, 4 channels of double ended 14-bit analog input, and 2 channels of 12-bit analog output.

A system layout is provided on in Figure 4.4. Two analog input channels were used to read the output signal of the rotary potentiometer indicating the location of the hydro handle, one digital input was used to read the position of the system engage switch, and two analog outputs were used to transmit an analog voltage to the machine controller, which indicated the desired location of the hydro handle according to the Simulink model.

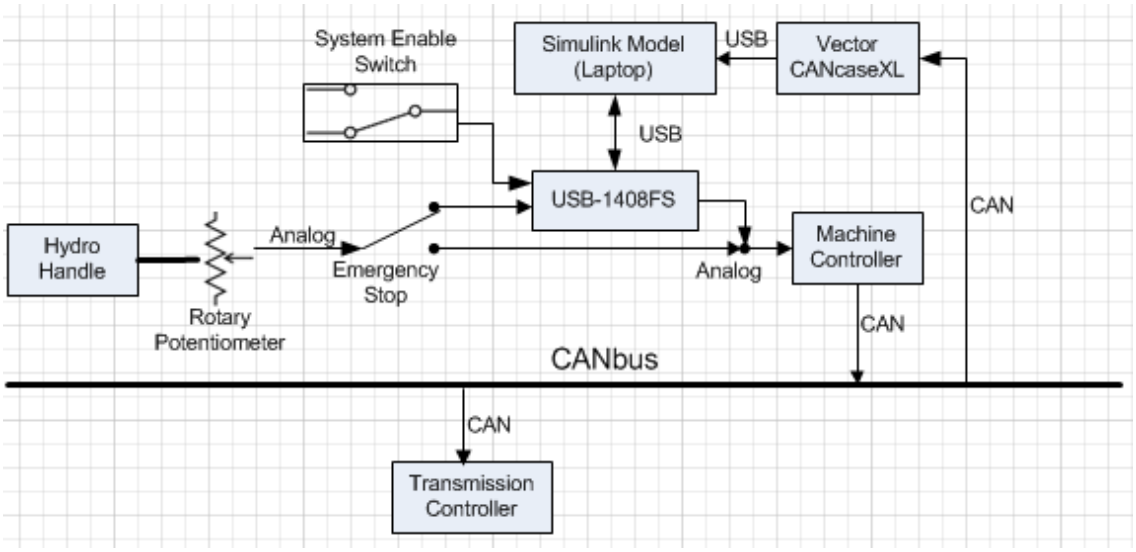

Figure 4.4: System layout for the control model running from Simulink

Additional machine information was provided to the Simulink model via a Vector CANcaseXL. The CANcaseXL directly interfaced with the laptop computer and the Simulink control model. The CANcaseXL made all CAN messages on the combine CANbus available to the model and also provided filtering capabilities to limit the messages input to the model. The CANcaseXL interfaced directly with Vector CANalyzer software, which was used for data logging.

In Table 4.1 the CAN signals input to the model for either control or data collection are given. All of the signals listed were easily accessible due to the standardization of nonproprietary CAN messages through the J1939 CAN standard.

Table 4.1: CAN signals input into Simulink model

PGN	Source Address	Message Rate	Signal Name	Start Bit	Length	Units
61443	0	20 Hz	Engine Percent Load At Current Speed	16	8	%
65256	28	5 Hz	Nav. Based Vehicle Speed	16	16	kph
65265	23	10 Hz	Wheel Based Vehicle Speed	8	16	kph
65266	0	10 Hz	Fuel Rate	0	16	L/h

All of the signals listed in Table 4.1 were part of messages with additional signals in each message. However, those signals were not relevant data, and were discarded. The 'Engine Percent Load At Current Speed' signal was limited to a data range of 0-100. This signal is a ratio of the current engine load to the rated engine power. It is important to note that due to the power bulge of an engine, additional power is available beyond the data limit of 100.

4.3.2. Control Design with the dSPACE MicroAutoBox

The dSPACE MicroAutoBox (MAB) is a stand-alone unit designed specifically for prototype model development. The MAB offered adequate I/O options with channels for Analog in/out, Digital in/out, and CAN.

The control model development for this system was done in MATLAB Simulink. MATLAB Simulink can load applications specific to the MAB, which allow Simulink to auto generate C code from Simulink models and directly load the generated file onto the MAB. Once a model has been loaded to the MAB, it begins running the model once power is supplied, just like an ECU. The MAB included ControlDesk, a software package that was used as a user interface software for diagnostics, data logging, and changing user inputs.

A system layout is provided on in Figure 4.5. Two analog input channels were used to read the output signal of the rotary potentiometer indicating the position of the hydro handle, one digital input was used to read the position of a system engage switch, and two analog outputs were used to transmit an analog voltage to the machine controller, which indicated the desired location of the hydro handle according to the control model. The MAB was connected to the combine CAN bus to receive machine information needed for data logging and control model inputs.

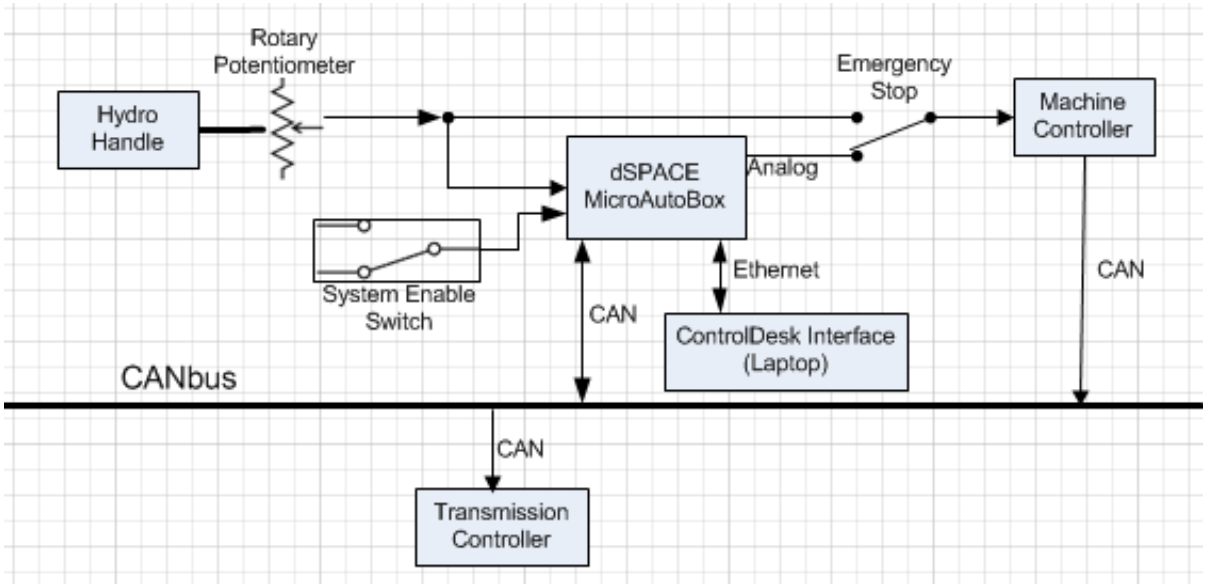

Figure 4.5: System layout for the control model running on the dSPACE MicroAutoBox

4.3.3. Grain Cart Velocity Input

To provide the model input requirement of grain cart velocity (described in section 5.2.2), tractor GPS velocity was wirelessly transmitted to the cab of the combine.

To accomplish this, two custom ECUs were built and programmed to be wired directly to wireless radios. The two ECUs used the identical hardware, but each had unique code specific to the system needs in each vehicle. The tractor GPS velocity is transmitted on the Tractor Implement Bus using standardized CAN message identification as specified in the CAN standard J1939. Table 4.2 specifies the message definition.

Table 4.2: CAN message used to receive tractor velocity

PGN	Source Address	Message Rate	Signal Name	Start Bit	Length	Units
65256	28	5 Hz	Compass Bearing	0	16	degrees
			Nav. Based Vehicle Speed	16	16	kph
			Pitch	32	16	degrees
			Altitude	48	16	meters

In order to transmit the tractor GPS wirelessly, the data was converted from CAN to serial data format. This conversion was done on a custom ECU which output serial data to a MaxStream XStream-PKG radio. The radio was used to both transmit data from the tractor cab and receive the data in the combine cab. Once the data was received in the combine cab,

it was converted back to CAN data format and placed on the combine bus. In order to avoid interference with messages transmitted from other ECUs on the combine bus, an open PGN (60416) and Source Address (126) were used to transmit the message with the same definition as it was received (Table 4.2) This process is summarized in Figure 4.6.

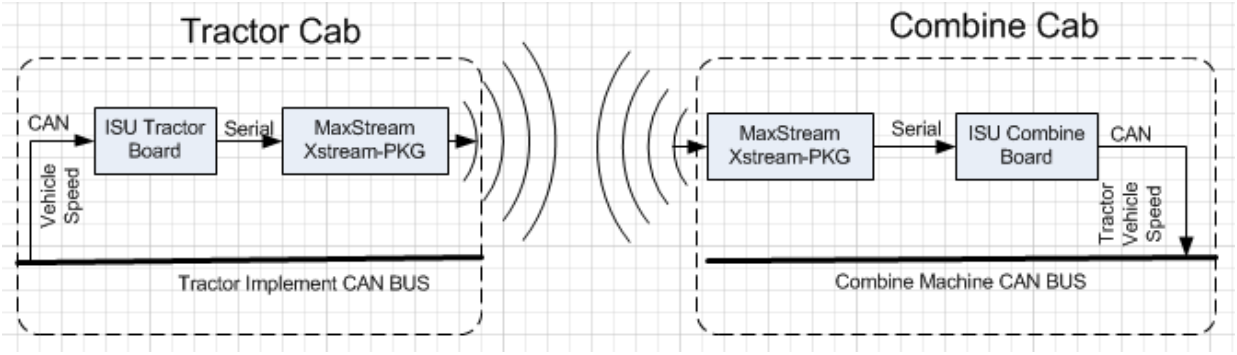

Figure 4.6: Wireless transmission of tractor GPS speed to the combine

4.3.4. Grain Cart Tracking

To track the location of both the front and back edges of the grain cart, a stereo camera based tracking system from the National Robotics Engineering Center (NREC) at Carnegie Mellon University was used. The tracking camera was mounted on the side of the combine near the grain tank (Figure 4.7).

Figure 4.7: Tracking camera mounted on the side of the combine.

The tracking camera provided image data to a laptop dedicated to processing the images. The images were processed and the x, y, and z coordinates of the front and back edge were output via serial data. Using the standard machinery coordinate definitions, x was parallel to

the path of travel, y was perpendicular to the path of travel, and z was vertical. The distance provided was the distance relative to the lens of the camera in units of cm.

In order to track the cart, targets were attached to the side of the cart. Three targets were used each with a unique design to indicate the front, middle, and back of the cart (Figure 4.8).

Figure 4.8: Grain cart with three targets installed for tracking

4.4. Results

The testing of the combine speed control system was completed outside of the grain harvest season, and all data presented in the two following sections was collected on a dirt test track.

4.4.1. Adjusting Combine Speed

In the test shown in Figure 4.9, a specific simulated hydro handle position was commanded from a Simulink model input. The result was a step input command received by the machine controller. It is important to understand that the ‘desired speed’ plotted was not a variable input into the control model, but rather a reference line that was added after the data collected. The ‘desired speed’ steps correlate to when the steps in the hydro handle were input, and the magnitude was dependent on the final steady state of the GPS speed. As shown, the speed adjustment method worked very well with quick and consistent response,

with minimal overshoot from the machine upon simulating an altered hydro handle position. Several tests similar to that shown in Figure 4.9 were conducted to ensure consistent and safe operation of the speed control.

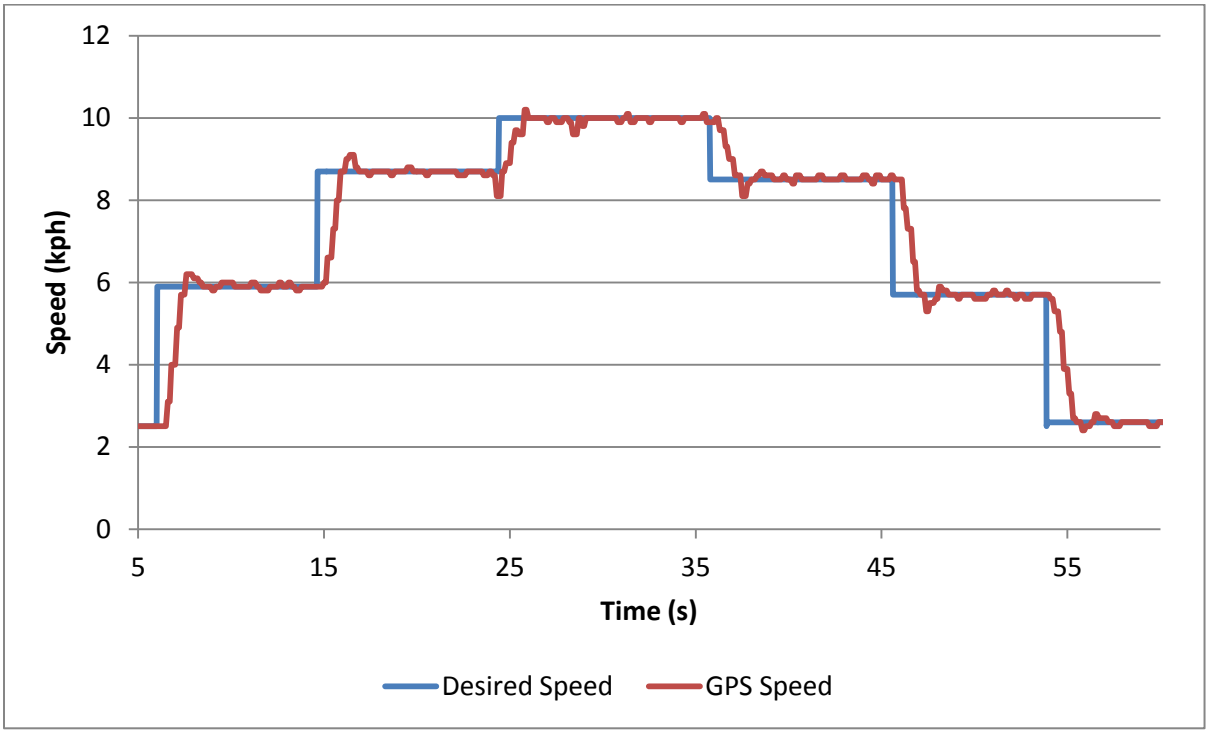

Figure 4.9: Plot of combine GPS and the step hydro handle command

4.4.2. Cart Position and Speed Input

The cart speed and relative position were successfully input into the control model. With the input signals of combine GPS speed, tractor (grain cart) GPS speed, and relative position, the accuracy of the cart tracking could be confirmed. It was assumed that both the combine GPS speed, and tractor GPS speed were accurate and that the paths of travel were parallel. The distance to the edge of the cart could be calculated using Equation 4.1 by summing the relative velocity and multiplying by the fixed time step of the model (in this case 0.2 seconds) as shown in Equation 4.1.

Equation 4.1: Distance to a cart edge

$$D_{cart\_edge} = D_i + \sum_{t=0}^{t_f} (v_{combine} - v_{tractor}) * \Delta t$$

The initial distance to a cart edge, D_i, was the distance input to the model when the cart was first detected at t = 0 s. Variables $v_{combine}$ and $v_{tractor}$ are the velocities of the tractor and combine used to calculate relative velocity. The output is the theoretical distance to a cart edge.

An example is shown in Figure 4.10. The distance plotted is the distance to the front edge of the cart. In this test, the cart was initially out of view of the tracking camera, and then approaches from the rear. While the cart is out of view, no tracking information can be provided. Once the cart enters the cameras field of view, a distance to the front edge is provided (t = 20.6) and the first data value provided is set as D_i in the edge calculation. In Figure 4.10 both positive and negative relative velocities are experienced throughout relative position range of approximately 10m. In all cases the real-time tracking data and the theoretical data provide nearly identical front x coordinate values which indicate a robust and accurate cart tracking system.

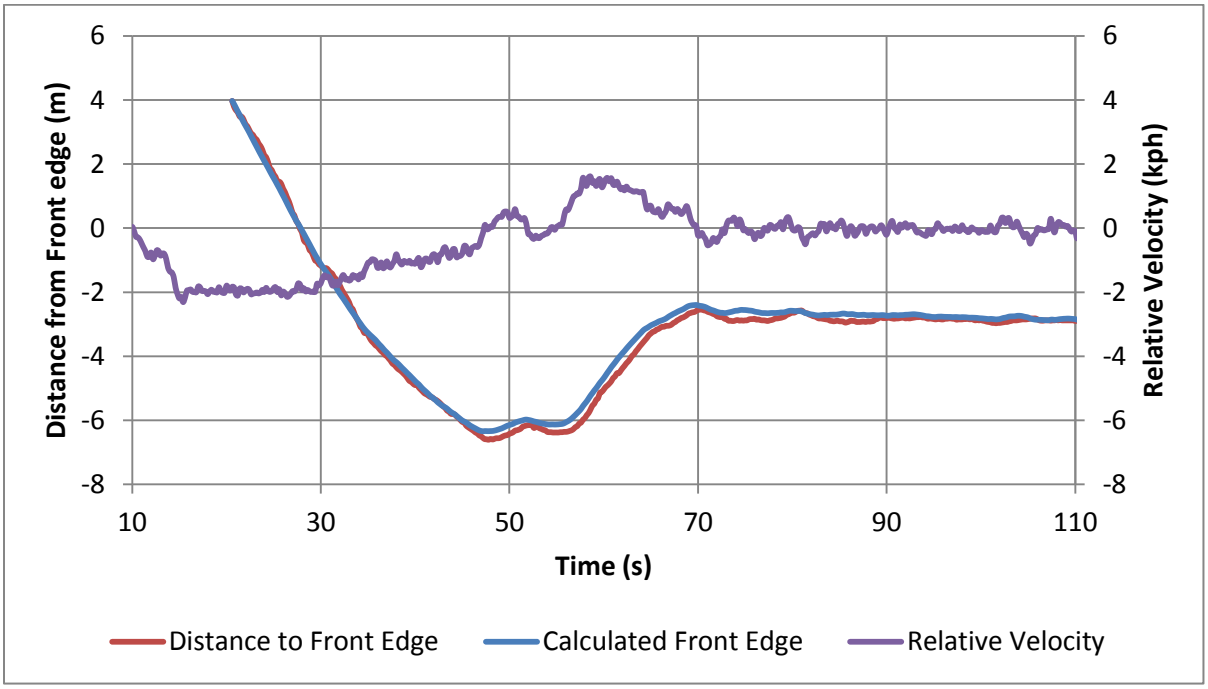

Figure 4.10: Plot indicating the accuracy of the NREC cart tracking

4.5. Conclusion

The objectives of this chapter were successfully met. The Simulink software platform proved to be adequate for model development and was easily compatible with the hardware platforms presented. In order to meet model input requirements of relative velocity and relative position, systems were either developed or integrated with to provide these inputs in a reliable manner. Through the test shown in Figure 4.10, these inputs were proven to be accurate. Through these components, speed control was successfully achieved. The systems proved to be a safe and reliable means of commanding the combine speed.

Chapter 5. Preliminary Control System Design

5.1. Introduction

The work of this chapter is primarily focused on the completion of objective 2. The feasibility of a combine relative position control system was investigated through a series of control systems using different inputs. The objective of these tests was to establish baseline relative positioning performance. The performance was evaluated based on the accuracy and responsiveness of the control system as well as machine response characteristics of engine loading and acceleration. With the knowledge gained from the different model inputs, several model features were developed and tested to improve performance and demonstrate the best possible control strategy architecture.

To successfully complete the goals of this chapter, data would need to be collected to demonstrate the control system's ability to meet the three performance metrics:

- Control relative position within ± 40 cm of desired location
- ΔP_{engine} <10%
- Rise time for a 3m shift in 14 seconds or less

5.2. Methods and Materials

5.2.1. Desired Ground Speed Input

Prior to the development of any position control, an assessment of the speed control and machine response times were made. This system used the hardware set described in section 4.3.1. The control model allowed the user to command a desired speed through an input of the Simulink model. The control model then used proportional control to command the simulated hydro handle position, which was output to the machine controller as an analog voltage, thus commanding a speed change.

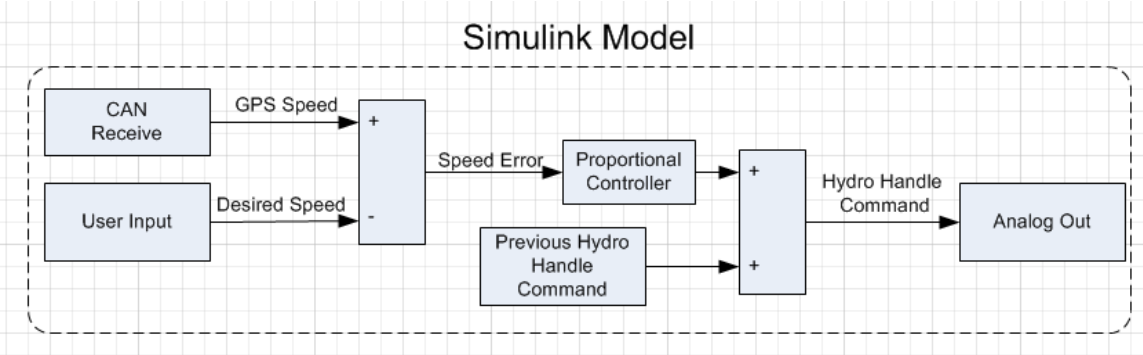

Figure 5.1: Model layout with desired speed as control input

5.2.2. Tractor Velocity Input

The hardware and system layout described in section 4.3.3 was used to input the tractor velocity into the control model. Calculating the relative position was achieved by summing the differential velocity of the combine to the tractor during fixed time steps. Upon system engagement, the model assumed a position error of 0. From that time forward, any relative velocity was used to calculate a total relative position error, as shown in Equation 5.1

Equation 5.1: Position error calculated from relative velocity

$$Error_{position} = \sum_{t=0}^{t_f} (v_{combine} - v_{tractor})\Delta_t$$

The control model used the input scheduling function which is described later in section 5.2.5. The controller using an error input of relative position used proportional derivative (PD) control to calculate control signal. Derivative control signal was added to avoid overshoot of the desired relative position. The controller using an error input of relative velocity used P control to calculate control signal. For relative velocity, P control only is sufficient because the control mode directly adjusts velocity.

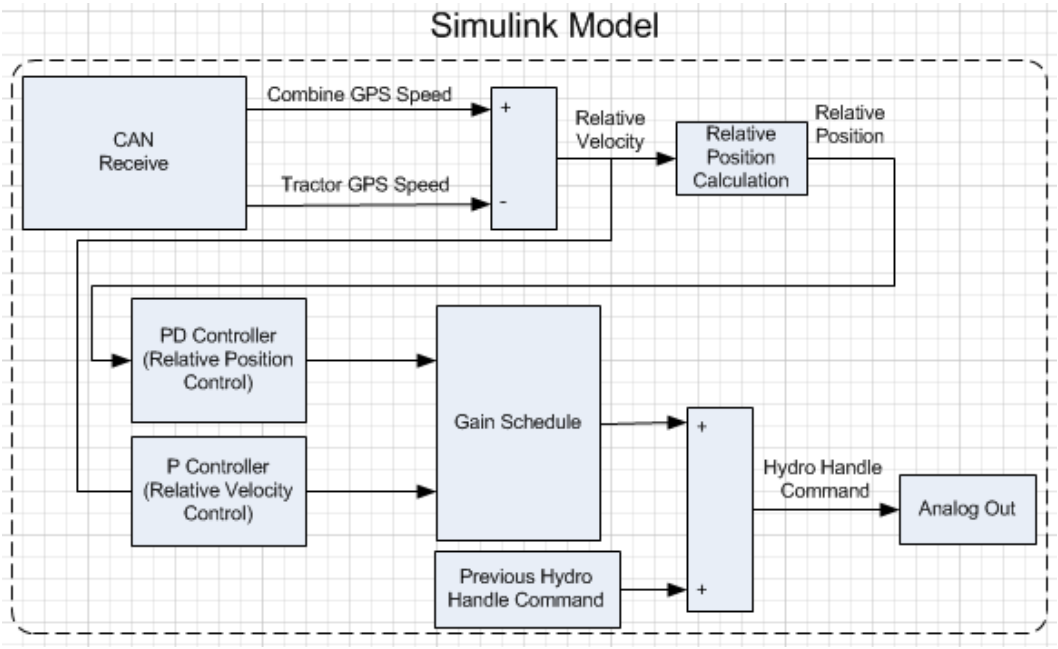

Figure 5.2: Model layout with relative velocity as a control input

5.2.3. Acceleration Limiting Model Feature

In order to limit the control signal required to achieve relative position shifts, a model development was made to limit the acceleration of the combine. The control signal is defined as the engine power, and the engine power consists of two components, a steady-state component, and a differential component:

Equation 5.2:

$$P_{engine} = P_{engine\_steady} + \Delta P_{engine}$$

The steady-state engine power, P_{engine_steady}, is the engine power required to maintain a constant speed immediately after achieving a desired speed. P_{engine_steady} is calculated by taking the average of the 'Engine Percent Load at Current Speed' CAN signal once the system reached steady state and up until the next step was commanded. The differential engine power, ΔP_{engine}, is the amount of additional power beyond P_{engine_steady} required to achieve the desired speed.

In order to achieve the $\Delta P_{engine} \leq 10\%$ metric, the magnitude of force, or acceleration, needed to achieve a desired step in ground speed, would need to be limited. The control model did not have the ability to directly control the rate at which the speed changes. Rather, the control model was designed to limit the rate at which the hydro handle location was moved forward or backward. This was implemented using a rate limiter from Simulink's block library which was added to the output of the model to provide maximum and minimum rates at which the position of the hydro handle could change.

5.2.4. Saturation Model Feature

In normal field operations, the combine operates within a tight range of speed to optimize machinery efficiency while preventing engine and separator overloading. To replicate this sort of machine control, a control model development was made which allowed the combine operator to input a minimum and maximum desired ground speed. With the ability to only control the position of the hydro handle rather than speed directly it was determined that precise speed control was not feasible for this project. Instead, the position of the hydro handle was held constant once either a minimum or maximum speed state was reached. Once inside the minimum or maximum speed limit state, the state was not exited until the control signal was exerted in the opposite direction. Control signal commands were used as exit conditions rather than speed because the combine ground speed will fluctuate due to terrain or harvest conditions even while the hydro handle position remains constant. The result was a system that was not expected to precisely control the maximum and minimum ground speed of the combine, but rather an allowable range in which the control model was allowed to adjust the position of the hydro handle. This model development was defined as the saturation model feature. The Stateflow diagram in Figure 5.3 shows the discrete operation states of the saturation model feature.

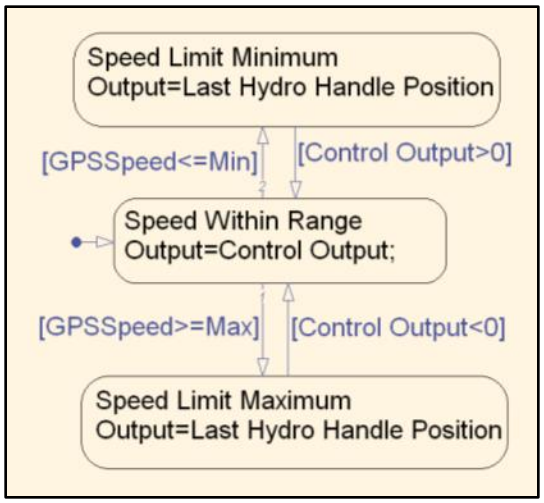

Figure 5.3: Saturation model feature Stateflow diagram

5.2.5. Input Scheduling Model Feature

In typical unloading-on-the-go field operations, the relative velocity of the combine to the grain cart is quite small (less than 1 mph). However, this relative velocity is constantly changing due to varying terrain, field conditions, and manually operated machine speed control. When the relative position error is large, the singular input of cart relative position error is a reliable means of control because the changes in relative velocity have a negligible impact on the control effort. As the error becomes small, controlling based on relative position becomes less effective due to lack of responsiveness to small changes in relative velocity. The lack of responsiveness is due to the fact that relative position control is based on errors already present. On the contrary, relative velocity as an error input offers the advantage of allowing the control system to predict a position error. For example, if the relative position error is 0, and the relative velocity is 0.5 mph, a relative position control system would exert no control signal, whereas the relative velocity control would immediately begin slowing the machine velocity because of the known error a relative velocity not equal to zero will induce. In order to optimize the control system to best use these inputs, a model development was completed where multiple inputs to the control model could be used to maximize the benefit of the each inputs response characteristics.

The implementation of the input scheduling used two discrete states, one controlling based on relative position, the other based on relative velocity. The transition between these two discrete states occurred at a position error of 40 cm, the desired relative position accuracy. A high-level Stateflow diagram of the gain scheduling is shown in Figure 5.4

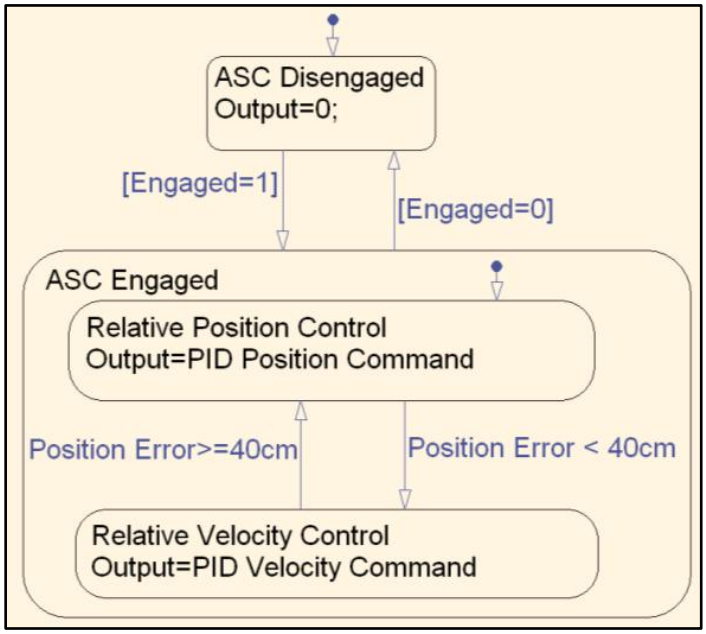

Figure 5.4: Input Scheduling Stateflow diagram

Two separate Embedded MATLAB functions were used in the Simulink model to determine the control signal required during each of these states as shown in Figure 5.5. These two functions used PID control and contained the identical internal code. The "Engaged" input was connected to a system enable switch. Upon engagement the block would output the necessary control to minimize input error, upon disengagement; the block output was held at zero. The remaining four inputs were for the PID function (P, I, and D gains as well as Error).

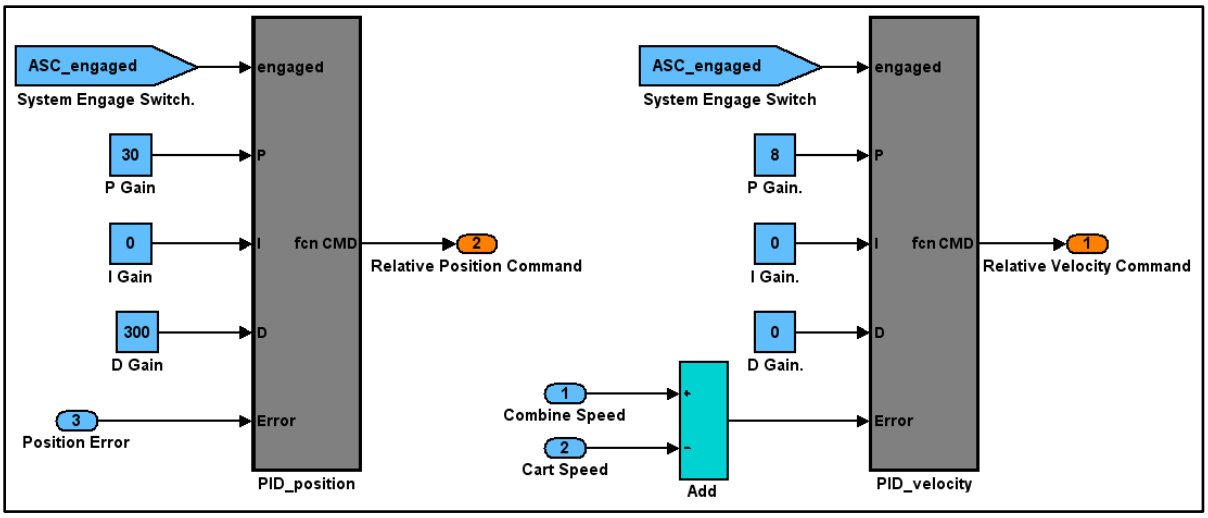

Figure 5.5: Embedded MATLAB Functions used for PID control

5.2.6. Gain Scheduling Model Feature

At small position errors, it was observed that the variance in relative position often resulted in highly variable D control signal. In the plot shown in Figure 5.6, the system was operating with small relative position error (<40cm) over a 30 second time period. During that time span the P control signal is shown to be relatively constant (proportional to error), while the D control signal is highly variable. When P and D are summed for PD control, the result is a control signal that is highly variable even while the relative position changes only by small amounts. The majority of this variability is a result of the D control signal. In order to smooth the control signal, a model development was made to schedule the gains at small relative position errors. The goal with this model development was to reduce or completely eliminate the variability attributed to the differential control signal.

Figure 5.6: Plot of P and D control signal with small relative position error (<40cm)

5.3. Results

5.3.1. Desired Ground Speed Input

The development and testing of the desired ground speed input was completed outside of the grain harvest season, and all data presented in this section was collected on a dirt test track. A typical result for the combine desired speed input model is shown in Figure 5.7. The controller was tuned to optimize the system for typical response characteristics, specifically a quick response time, and small overshoot were desired.

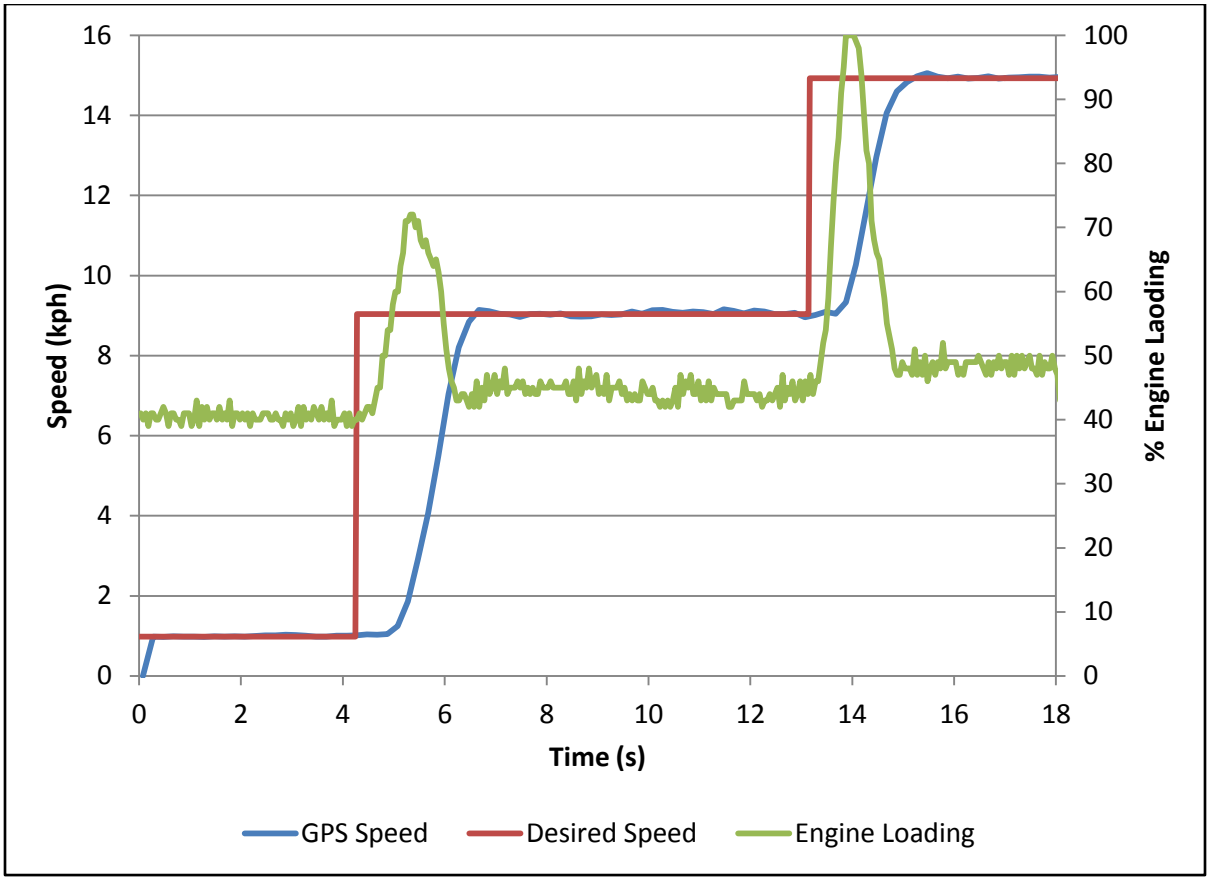

Figure 5.7: Step response to commanded speed changes

Table 5.1: Step Response characteristics of plot shown in Figure 5.7

Step range (kph)	Start time (s)	Rise time (0%-100%)	Overshoot (%)	ΔP_{engine} (%)	Maximum Acceleration (kph/s)
1-9	4.24	2.23	1.4	28	5.3
9-14.9	13.07	2.02	2.4	52	4.7

No specific metrics were set for this exploratory stage of the project. Both rise time, and overshoot (values given in Table 5.1) were better than expected and considered more than adequate for the desired control. Although the response was very good, the change in engine load due to the speed change (ΔP_{engine}) was very high. This test documented the most rapid machine response possible.

Tests were also completed with the desired speed input to quantify the delay time of the machine response. The delay time of the machine was defined as the difference between a step input of the position of the hydro handle, and when the speed of the machine began to increase (Figure 5.8). This delay time was important to understand because it was an unavoidable physical constraint that attributed to delay in the response time of the control system.

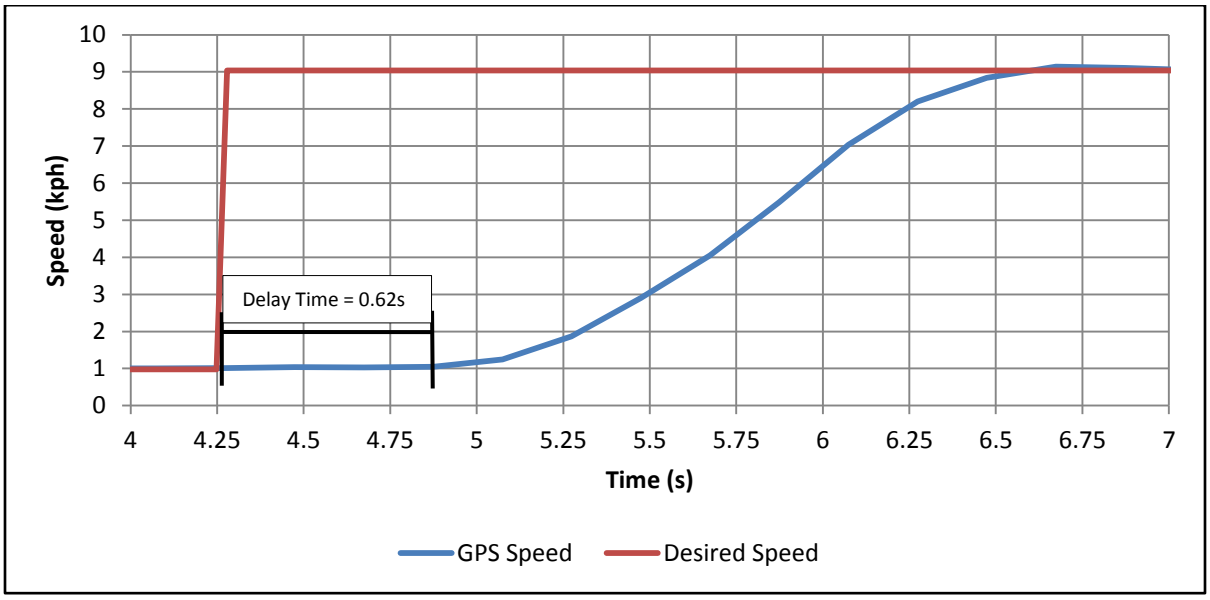

Figure 5.8: Typical speed command step response

A series of tests were performed at wide range of initial ground speeds (0.4-15 kph) and both positive and negative speed step commands were given. The results are listed in Table 5.2.

Table 5.2: Machine delay in speed response

Initial Speed (kph)	Delay Time (s)	Positive Step	Negative Step
0.4	0.54	X	
1.0	0.54	X	
1.0	0.63	X	
2.5	0.50	X	
5.4	0.53		X
5.9	0.48	X	
5.9	0.35		X
8.7	0.61	X	
8.7	0.51		X
9.0	0.60		X
10.0	0.45		X
15.0	0.52		X

From the results listed in Table 5.2, the delay time average and standard deviation for the positive step, negative step, and combine total were calculated (Table 5.3). With the GPS speed CAN message updating at a rate of only 5 Hz, much of the variation can be attributed to signal delay. Although it was important to recognize this physical constraint of the system, it was determined that an average delay in response of 0.52 s would not significantly hinder development or impact final performance.

Table 5.3: Machine delay in speed response

Speed Change Direction	Average Delay Time (s)	Standard Deviation (s)
Positive	0.55	0.05
Negative	0.49	0.08
Combined	0.52	0.07

5.3.2. Acceleration Limiting Model Feature

The development and testing of the acceleration limiting model feature was completed outside of the grain harvest season, and all data presented in this section was collected on a dirt test track. A typical result for the acceleration limiting model is shown in Figure 5.9. The response characteristics for the step responses shown are given in Table 5.4.

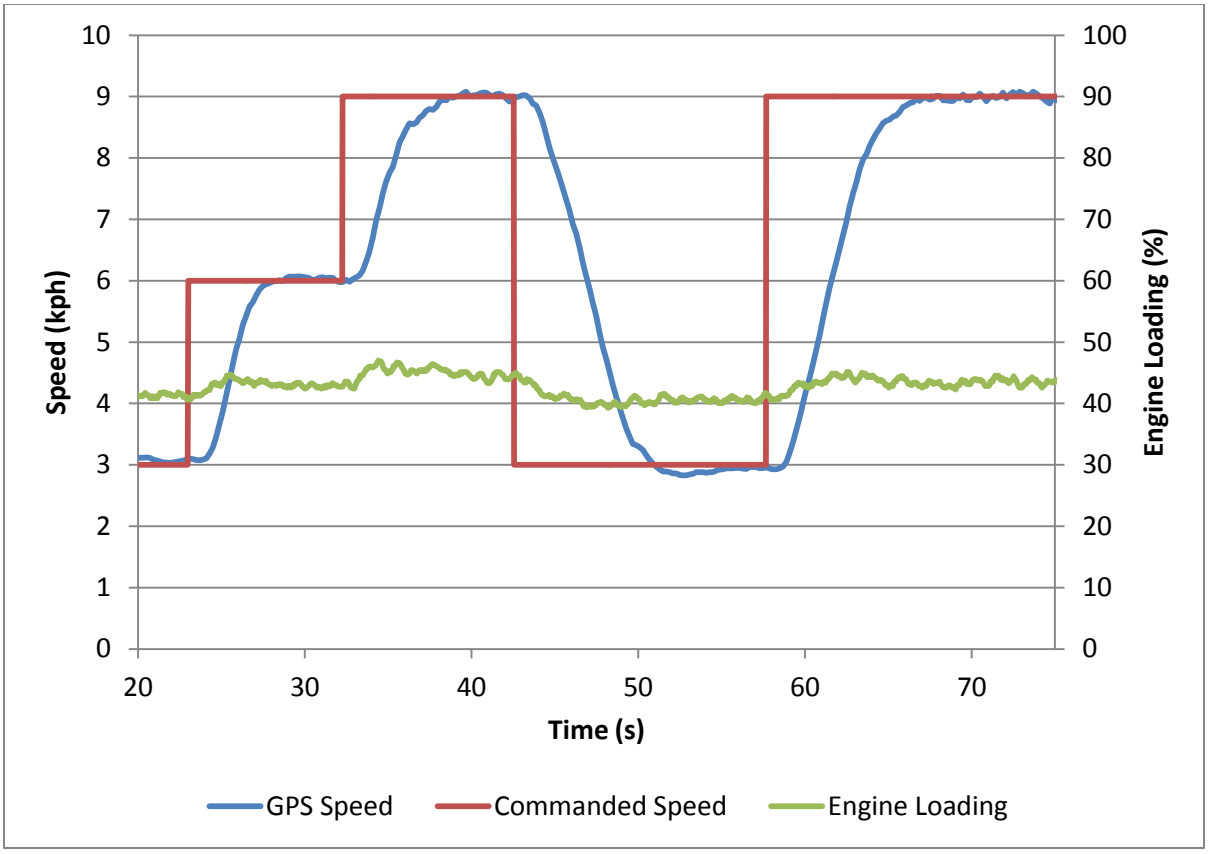

Figure 5.9: Step response characteristics with acceleration limiting control model

Table 5.4: Step Response characteristics of plot shown in Figure 5.9

Step range (kph)	Start time (s)	Rise time (0%-100%)	Overshoot (%)	ΔP_{engine} (%)	Maximum Acceleration (kph/s)
3-6	23.01	5.47	2.3	2	1.0
6-9	32.26	6.82	-	3.1	.95
9-3	42.56	8.41	2.8	-	-.96
3-9	57.68	11.7	-	3.9	1.1

The response times were much slower than the control model without acceleration limiting, with the maximum acceleration values approximately five times lower. The acceleration limiting did succeed in dramatically reducing the ΔP_{engine}. The difference in response is clear to see in Figure 5.10, which gives a comparison between the two systems responding to a step input of a desired speed of 9 kph. The resulting data from acceleration

limiting model feature provided the information needed to satisfy the requirements of the $\Delta P_{engine} \leq 10$ metric.

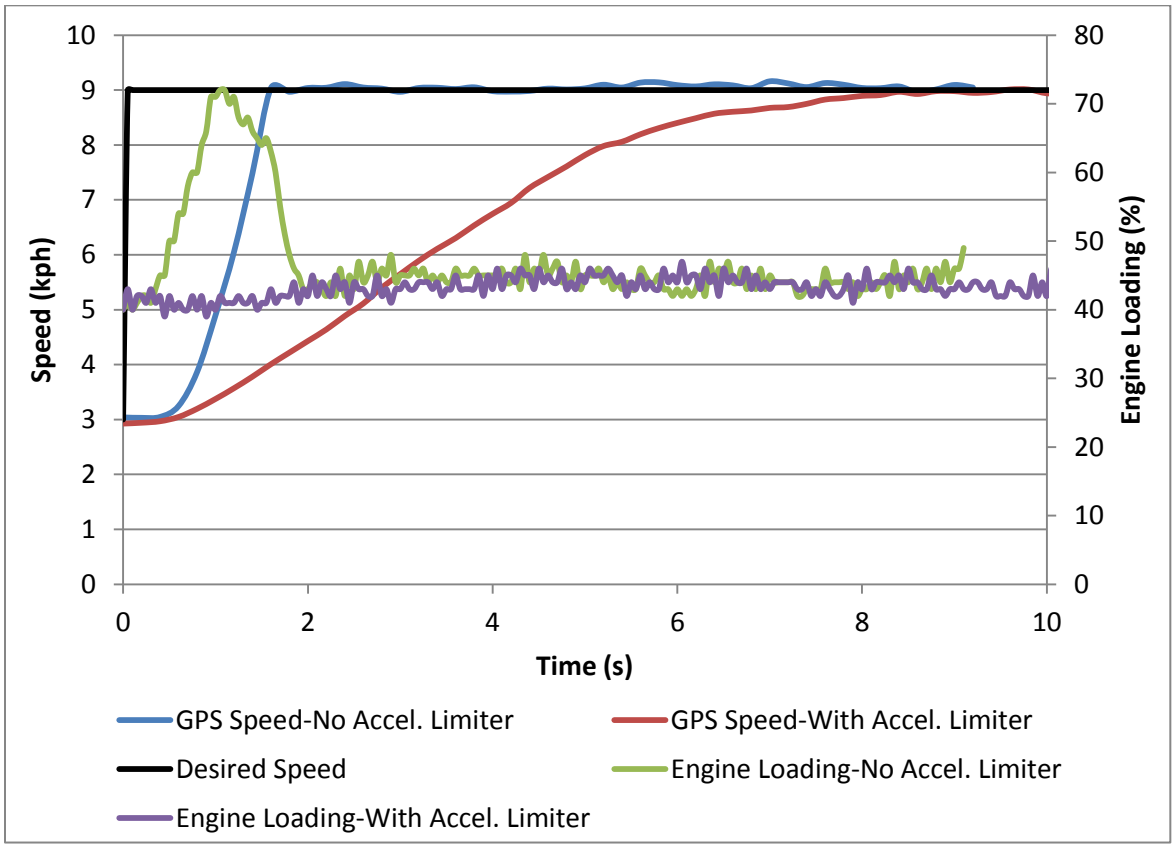

Figure 5.10: Comparison of model response with and without acceleration limiter

In addition, the acceleration limiting function served to increase operator comfort with the system by decreasing the amount of detectable acceleration. A study done by the University Hospital Maastricht of the Netherlands found the acceleration detection threshold for anterior-posterior (fore-aft) movement to be 9.7 cm/s^2 (0.35 kph/s) (Kingma 2005). Although this threshold is still lower than the maximum acceleration values observed with the acceleration limiting function enabled (approximately 1 kph/s), they are much closer to the threshold than the maximum acceleration values observed with the acceleration model feature disabled (approximately 5 kph/s). In addition, it is believed that a machine operator's acceleration detection threshold would be higher than that found in the study due to machine vibrations and travel over uneven terrain.

5.3.3. Relative Velocity Input and Input Scheduling Model Feature

The development and testing of the relative velocity input and input scheduling model feature was completed outside of the grain harvest season, and all data presented in this section was collected on a dirt test track. A typical result for this control system is shown in Figure 5.11. In this test case the system was enabled at t = 110 s, which set the relative position error to 0 m. In order to induce relative position error into the system, the lead vehicle rapidly increased speed by a fixed speed step. The tractor used (John Deere 8230R) featured an infinitely variable transmission (IVT) which allowed the tractor operator to easily command changes in a desired speed set point. In the test, the tractor began at 1 mph and steps were in 1 mph increments up to 5 mph. For unit consistency, all speeds (mph) were converted to metric units (kph) in the plot shown in Figure 5.11.

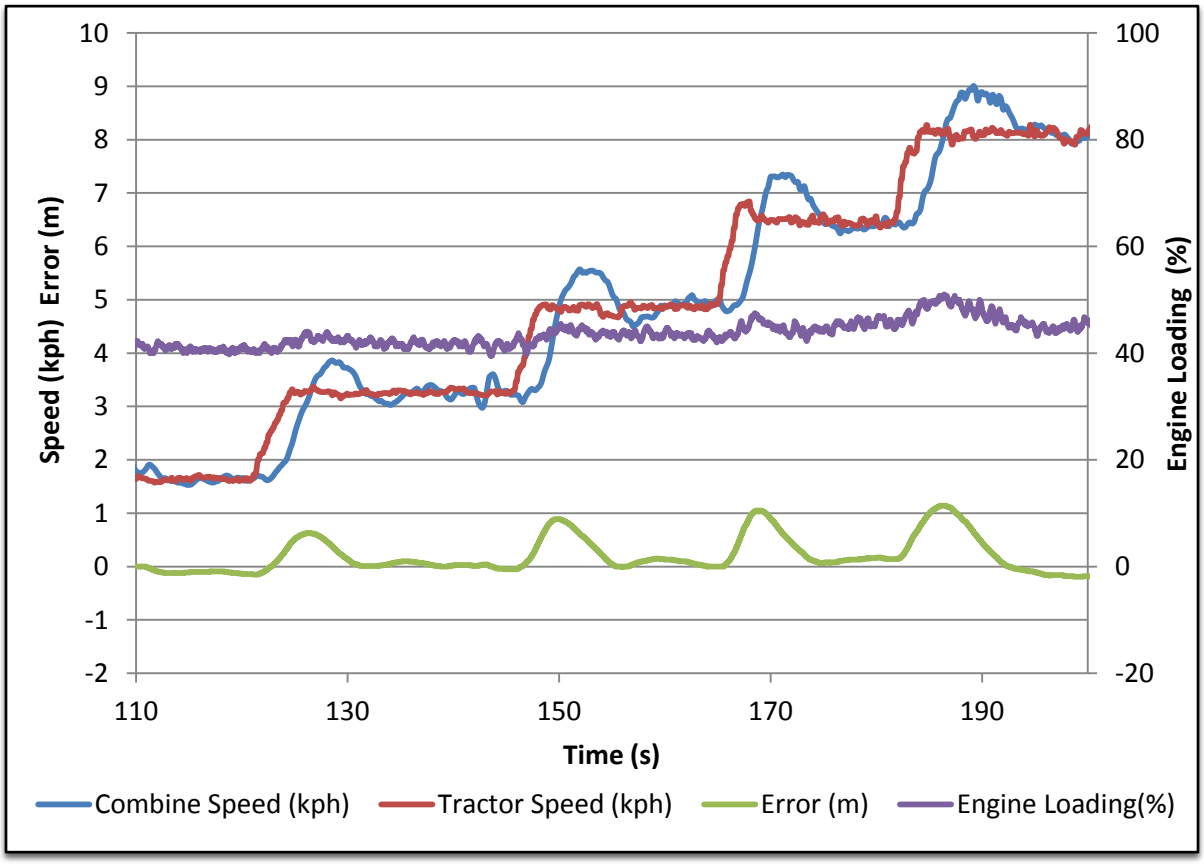

Figure 5.11: Response for control model using relative velocity

Response characteristics are given in Table 5.5. The rise time is the span of time from the start time of the speed step until the error returns to zero. In these tests the ΔP_{engine} metric was satisfied as well as desired response times.

Table 5.5: Step Response characteristics of plot shown in Figure 5.11

Step range (kph)	Start time(s)	Rise time (0%-100%)(s)	ΔP_{engine} (%)	Maximum Acceleration (kph/s)
1-2	121.2	9.83	2	0.64
2-3	145.21	10.14	1.75	1.02
3-4	164.71	10.46	3.25	1.01
4-5	181.81	10.58	6	0.68

The input scheduling was successful in generating a control system that had desirable response characteristics at both large and small magnitude relative position errors. Upon examination of the data it was clear to see the positive impact of the input scheduling, as shown in Figure 5.12. In the plot a relative position step input of +3m is given near t = 180 s. From t = 180-190 s, the input scheduling uses the position based control and the control signal begins as a large positive and decrease as the machine approaches the desired position. At t = 190 s (position error = 40 cm) the inputs are switched, and control signal significantly decreases to minimize the relative velocity, and succeeds in matching the tractor velocity in approximately 2 seconds. If the relative position control would have remained as the control input, significant overshoot would have occurred. The only way to avoid this overshoot would be to decrease the P gain, which would have increased response time. Instead, with relative velocity as the control input once the position error was less than 40 cm, the relative velocity was rapidly decreased resulting in precise relative position control and an overshoot of only 17 cm.

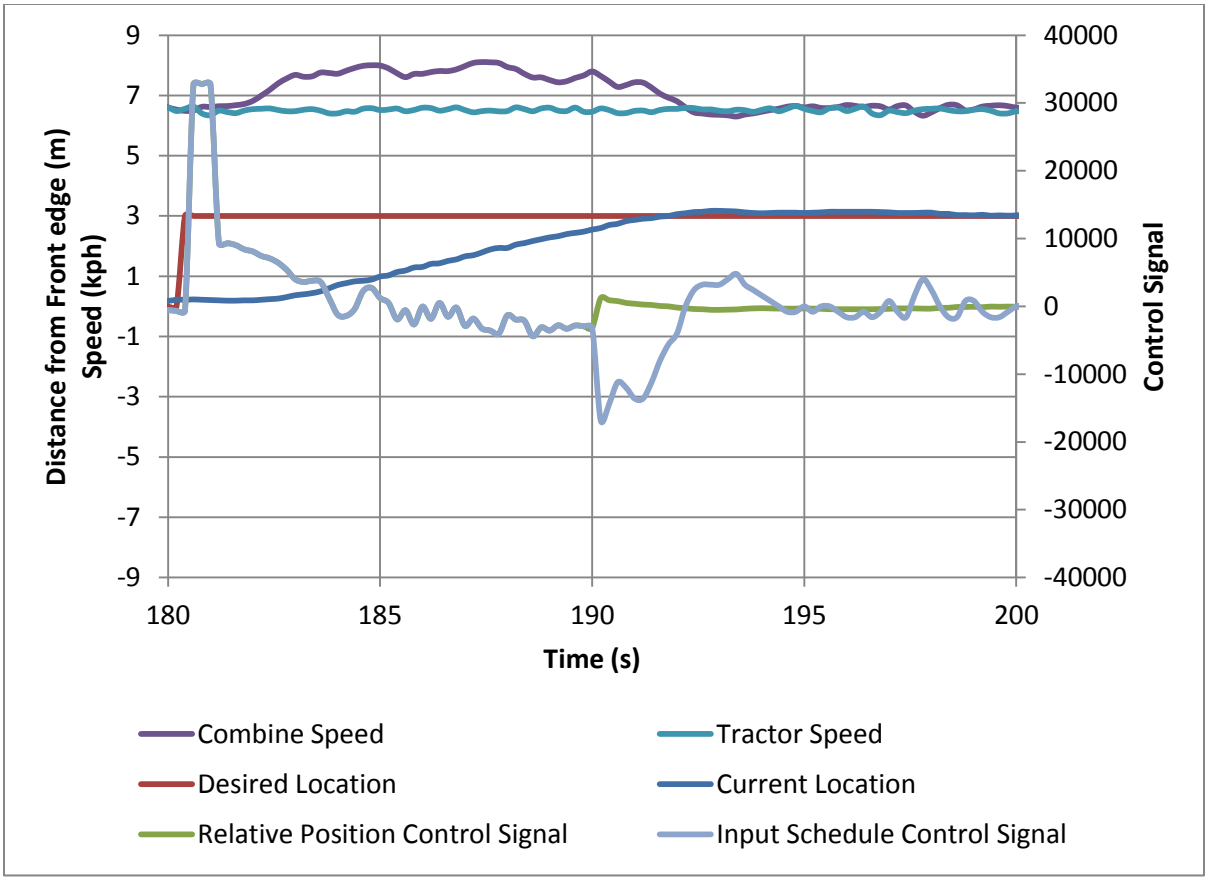

Figure 5.12: Input scheduling enabled at a relative position error of 40 cm.

One detail not shown in data is the error that accumulated between the calculated relative position and the actual relative position. Relative position error would accumulate in this system because of small differences in the GPS speed of the tractor and the combine. Any difference between the two GPS systems was an error in relative velocity, which was summed to produce the relative position. After the control model would run for a several minutes a visible error in the relative position was accumulated. Although it was very difficult to measure the exact size of this error, Figure 5.13 provides a plot in which the tractor and combine were parked side by side, where the true vehicle speed is 0 kph. Although the errors in speed are small, in 11 seconds the calculated position error was 35 cm, while neither vehicle had physically moved.

The error in the tractor velocity was typically higher than that of the combine, which was attributed to different levels of GPS signal accuracy. The tractor GPS receiver used the

John Deere SF1 signal while the combine receiver used the higher quality John Deere SF2 signal. Both signals were received using John Deere Starfire iTC receivers.

Figure 5.13: Calculated position error while both vehicles are stationary

Valuable control model development was still completed using this input. However, the accumulated position error indicated the necessity of having a real-time cart tracking system as part of the final solution for relative cart positioning.

5.3.4. Saturation Model Feature

The development and testing of the saturation model feature was completed during the grain harvest season, and all data presented in this section was collected while harvesting crop in normal field conditions. The saturation model feature worked to prevent large speed changes and deviations from the desired speed, but it did not provide precise control of the minimum and maximum speeds due to the delay in drivetrain speed response discussed in 5.3.1. In Figure 5.14 an example in which the speed limit is reached for both the maximum (8.37 kph, 5.20 mph) and the minimum (7.72 kph, 4.8 mph) as the control model makes both positive and negative relative position shifts. At t = 51.2 s, the combine reaches the maximum speed and the position of the hydro handle is saturated (80% forward), but due to

the delayed response in the drivetrain, the speed continues to increase another 0.73 kph (0.45 mph). Similarly, at t = 100.6 s, the minimum speed is reached and the position of the hydro handle is saturated (70% forward), but due to the delay in response of the drivetrain, the speed continues to decrease another 0.54 kph (0.34 mph).

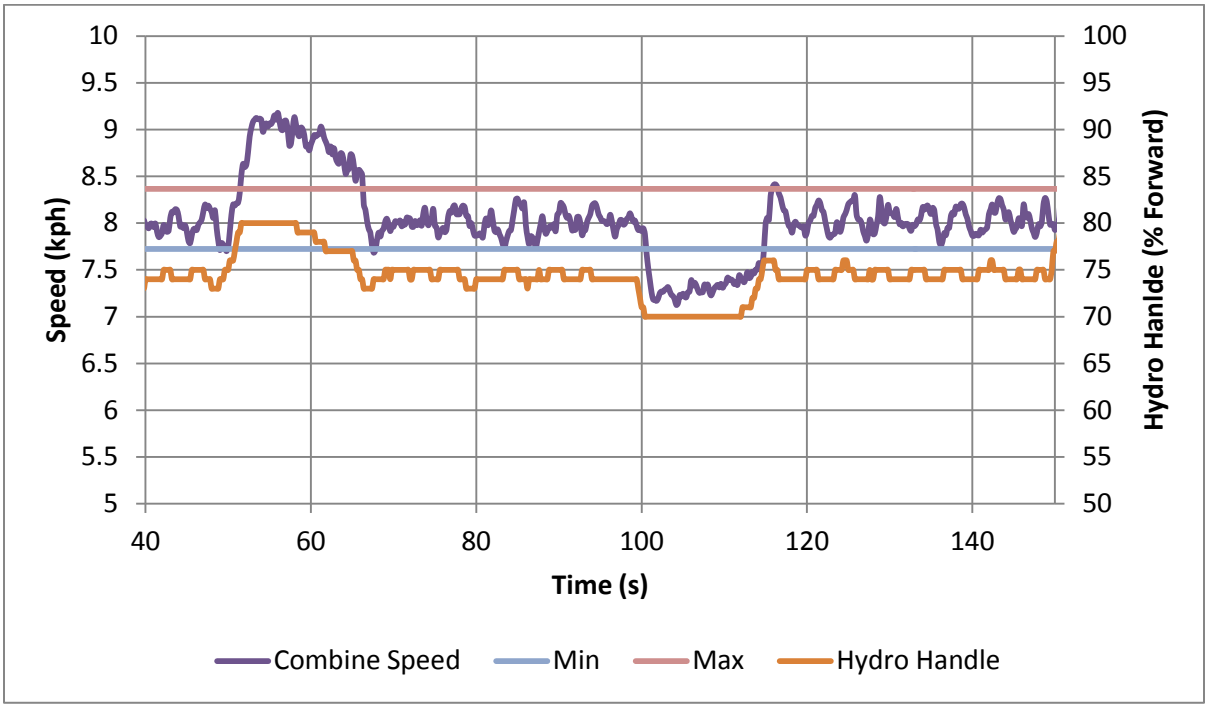

Figure 5.14: Saturation model feature for a range of 8.0±0.32 kph (5.0±0.2 mph)

The overshoot of the speed limits was an issue in every test case where the maximum or minimum speed was reached, but the size of the overshoot was largely dependent on the magnitude of the acceleration when the speed limit point was reached. Although this model feature was not extremely precise, it was successful for protecting the machine from excessive speed change commands during the operation of the active speed control system.

5.3.5. Gain Scheduling Model Feature

The development and testing of the gain scheduling model feature was completed during the grain harvest season, and all data presented in this section was collected while harvesting crop in normal field conditions. The gain scheduling model feature was setup to use PD control for relative position errors greater than a magnitude of 50 cm. For errors of magnitude smaller than 50 cm, D control was eliminated completely in order to provide the more stable control characteristics of P control. The gains used for P and D were based on the

gain value analysis completed in section 6.3.1. Based on this analysis, the recommended P gain value of 30 and D gain value of 300 were used. A typical result for the model development using the gain scheduling is shown in Figure 5.15. In order to monitor the effects of the gain scheduling feature, the input data was replayed back into the control model using the control model without gain scheduling. The difference between the control signal of these two models was plotted as "Control Signal Difference" in Figure 5.15 and was equal to the control signal of the model with gain scheduling minus the model without gain scheduling. Upon the step input of a 3 m change in desired location, the response of the two models is identical up until t = 128 s. At t = 128 s, the relative position error reaches the gain scheduling transition of 50 cm, which results in different control signal. The control signal of the system using gain scheduling was a small negative due to the negative relative position, but the system without gain scheduling had a positive control power due to the large D control signal attributed to matching the relative velocities.

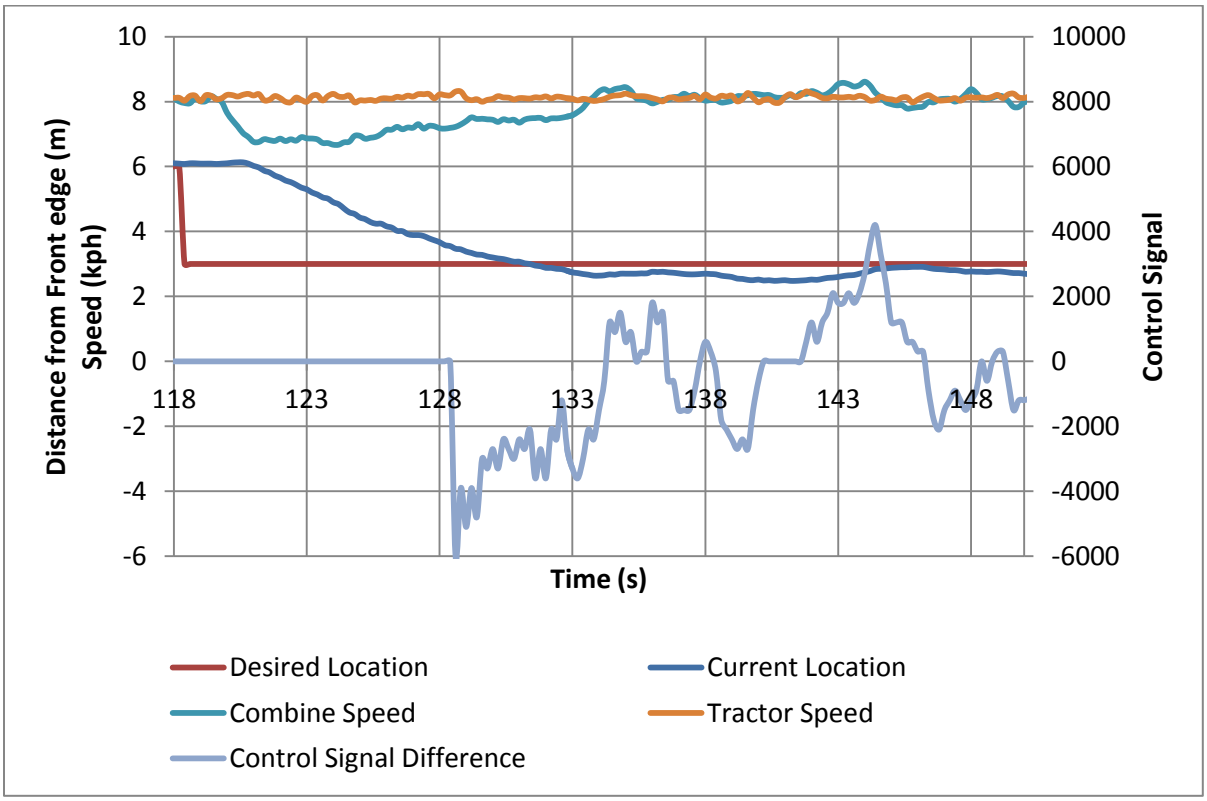

Figure 5.15: Plot of difference between control signal of models with and without gain scheduling

The gain scheduling control model functioned correctly, but the response it produced was less desirable than the control model without gain scheduling. The gain scheduling resulted in a response that would consistently overshoot the desired location. This overshoot was due to the P control exerting control power in the direction of the error, even when the error was small and the relative velocity large. At t = 128 s in Figure 5.15 the effects of the gain scheduling are evident, where the relative velocity is being minimized prior to t = 128 s, but at t = 128 s the control power is exerted to increase the relative velocity due to the gain scheduling. It is not until t = 132 s that the P control power begins decreasing the relative velocity due to a negative position error. The delayed control action to minimize the relative velocity resulted in an overshoot of the desired location by 38 cm. Although the exact response of the other control model cannot be known, it is predicted to have a smaller overshoot due to the difference in control power shown after t = 128 s.

The difference between the control models with and without gain scheduling was evident in the results from the field testing completed. In Figure 5.16 an interval plot is shown for control with (1) and without (0) gain scheduling, plotted versus the maximum overshoot. In some tests of the control model without gain scheduling the desired location was never reached due to the D-gain for the control model without gain scheduling. In these cases, this undershoot was recorded as a negative overshoot.

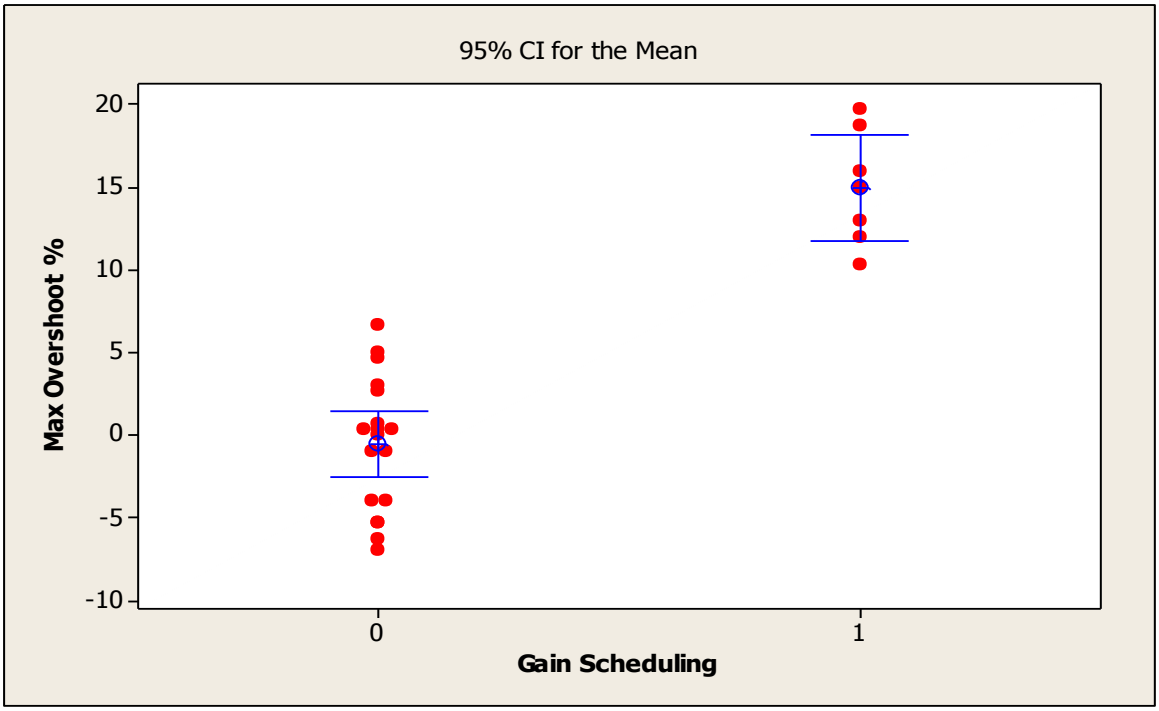

Figure 5.16: Interval plot of Gain Scheduling vs. Maximum Overshoot

The gain scheduling had a statistically significant impact on the maximum overshoot, with a P-value of 0.000. The average and standard deviation overshoot (μ,σ) of the control model running without gain scheduling (0) was -0.57% , 4.07% whereas the overshoot of the control model running with gain scheduling (1) was 14.95% , 3.45%. Although the gain scheduling did succeed in eliminating the derivative gain at small relative position errors, the end result was a control system with significantly reduced control accuracy.

In order to improve the gain scheduling feature, further development would be recommended to make the gain schedule a composite of the two gain types as opposed to the discrete approach that was taken. In this composite gain schedule, instead of completely eliminating the derivative gain at a position error of 50 cm, the percentage of the derivative gain used in the control signal would be decreased at a linear rate as the position error continued to decrease. It is assumed that this composite gain schedule would decrease the impact of the highly variable derivative gain at small position errors, while still avoiding overshoot.

5.4. Conclusions

From the various inputs and model features presented in this chapter, several conclusions can be drawn and a recommendation made for the ideal control strategy architecture to be used as the final combine active speed control model, and which successfully completes the requirements of objective 2 presented in Chapter 3.

The ground speed input provided the information necessary to gain a basic understanding of machine response characteristics. The data provided the information necessary to understand the physical delays of the system as well as the impact of rapid speed changes on engine load. The acceleration limiting model feature was designed to limit the ΔP_{engine} due to speed changes and the model feature successfully accomplished that goal. The acceleration limiting model feature did significantly reduce response time, but it was believed that the response metric set in the introduction of this chapter was still feasible.

The relative velocity model input provided the information necessary to provide inputs that allowed the control model to accurately achieve a relative position. Due to the addition of this model input, the control model was able to quickly respond to changes in speed of either vehicle which greatly improved the system performance when operating with small relative position errors. In addition, the relative velocity input allowed the input scheduling model feature to be created which eliminated overshoot due to relative position based control and gave a model response that met the accuracy metric of ±40cm.

The saturation model feature worked as designed and did successfully prevent large changes in the ground speed of the combine. Although, there was variation in peak ground speed, the model feature was adequate for the requirements of this project.

The gain scheduling model feature worked as designed, but the performance was not at an acceptable level for continued use in the final control system, as the overshoot often exceeded the accuracy metric of ±40 cm. Although the purpose of the gain scheduling is still valid, the model feature would need to have the improvements mentioned in section 5.3.5 prior to implementation.

The models and data collected in this preliminary design provided the knowledge needed to determine the feasibility of the project and what performance levels could be expected in the final design. The results of these tests met the objectives listed in the beginning of the

chapter and provided sufficient data to design a robust final control system. Following the completion of the Chapter 5 goals, it was determined that the final control system should use both relative position and velocity as model inputs, the acceleration limiting, input scheduling, and saturation model features.

Chapter 6. Final Control System Design and Testing

6.1. Introduction

The final control system design was done on the MicroAutoBox, as described in section 4.3.2. This system was used because of the ability to integrate with the NREC cart tracking system. The final control system was designed using the three metrics listed below. In order to avoid the input scheduling model development impacting data quality (input scheduling occurred at ± 40 cm), response time was defined as the rise time only when the relative position error was an input, known to be from 0.4 m-2.6 m for the 3 m step size. Therefore the response time was defined as rise time (13.3%-86.7%), which accounted for 73.4% of response and in Figure 6.1. In order to account for this change, the required time to achieve this percent of the shift was adjusted from 14 to 10 seconds.

- Control relative position within ± 40 cm of desired location
- ΔP_{engine} <10%
- Rise time (13.3%-86.7%) for a 3m shift in 10 seconds or less

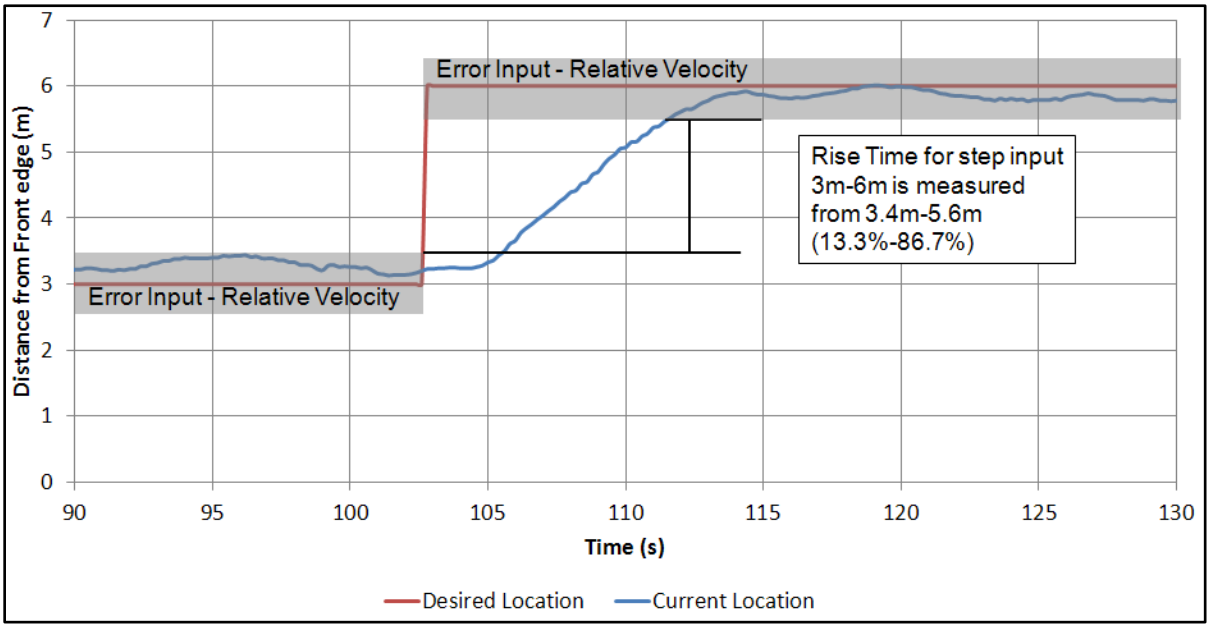

The focus of this chapter was to complete the third and final research objective, which required the system performance to be validated in normal field conditions. The model was developed using the knowledge gained from the preliminary control design and results.

Following tuning of the control system gains both in and out of crop situations; the system performance was then evaluated in crop. In order to analyze the system performance, the following treatment factors were used:

- Desired Speed and Engine Loading
- Ranges of the Saturation Model Feature
- Direction of Relative Position Commands

6.2. Methods and Materials

6.2.1. Final Control System Design

The final control system development was heavily based on the knowledge gained from the data of testing the preliminary control system. The control model ran on the MAB (4.3.2) and used the NREC cart tracking system (4.3.4) and the tractor and combine GPS velocity were used to calculate the relative velocity input (4.3.3). The model used the acceleration rate limiter (5.2.3) to achieve the ΔP_{engine} <10% metric. The model also used the input scheduling model feature to optimize response (5.2.5). A system layout is provided in Figure 6.1.

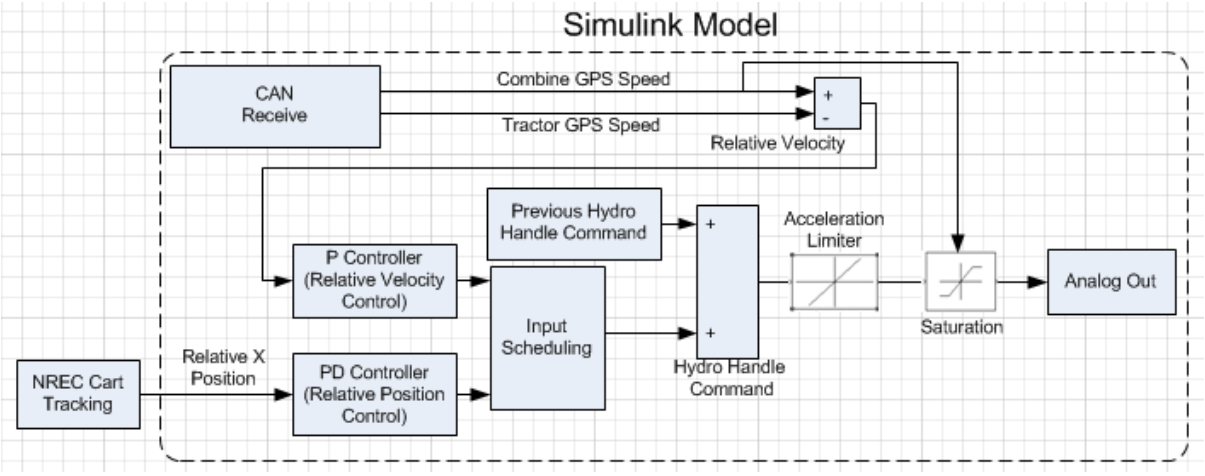

Figure 6.1: Final Control Model Layout

6.2.2. Desired Speed and Engine Loading

The amount of load placed on the engine was believed to impact the ability of the machine to accelerate and change speeds because of limited power availability. The load

placed on the engine is not a parameter that is easily or accurately controlled due to continuously changing crop and terrain conditions while harvesting. In order to test this parameter, relative position step inputs were given at three discrete speeds 3.0, 4.0 and 5.0 mph. For unit consistency, these speeds were converted to metric units (4.8 kph, 6.4 kph, and 8.0 kph). 3 meter step inputs were used for all repetitions and the saturation range limit was set to 1.6 kph (1 mph). The following hypothesis was tested:

- As the average engine load increases the rise time will also increase.

6.2.3. Saturation Model Feature

The saturation model feature was applied in all field tests to avoid overloading the engine and crop separator. The saturation was enabled at three discrete levels above and below the desired speed: ±0.32 kph, ±0.8 kph, and ±1.6 kph (0.2 mph, 0.5 mph, and 1.0 mph). Although the control model could not directly limit the combine ground speed, by holding the hydro handle position constant once the limit was reached, the following three hypotheses were tested:

- As the range of the saturation model feature increases, the ΔP_{engine} observed during a step input will also increase.
- As the range of saturation model feature increases, steady state error will also increase.
- As the range of the saturation model feature increases, the rise time will decrease.

6.2.4. Direction of Relative Position Command

The direction in which the relative position commands were given was alternated between forward and reverse commands with an equal magnitude of 3.0 m. This was done with the intent of gaining knowledge on the impacts of accelerating and decelerating the machine while harvesting crop. Although the control model was developed and tuned to limit the impact of the model commands on the engine load, it was expected that the effects of relative positioning would still be evident in both the engine load data as well as rise time. For the engine load data it was known that accelerations (positive relative position commands) would produce a positive ΔP_{engine} and decelerations (negative relative position

commands) would produce a negative ΔP_{engine} so no hypothesis was set to be tested; rather, a simple statistical analysis of the data to indicate the magnitude and variations of ΔP_{engine} during the step inputs would be completed. In all of these tests the control range limit was held constant at ±1.6 kph (1.0 mph). The following hypothesis was formed to test the rise time:

- The relative position shifts given in the forward direction will have a slower rise time than those given in the reverse direction.

6.3. Results

6.3.1. Control Gains

When tuning the gains of the controller, a wide range of values were tested. Many of these gain values resulted in either an extremely under or over damped system response. In these cases, the NREC cart tracking would not function because the targets would exit the camera's field of view, and the test would be aborted. In between these extremes, a range for both the proportional and derivative gains was identified that would result in a control system that could maintain a relative position of the combine that allowed the NREC cart tracking system to function.

The following two sections are the data that was collected while inside the functional ranges. All tests were conducted using a relative position shift step input of +3m. Only forward relative positions shifts were tested because this was identified to be the more difficult test condition due to the required machine acceleration. The data presented is intended to be a justification for the proportional and derivative gains used in the control model.

6.3.1.1. Proportional Gain Tuning

For the tests to determine the optimum proportional gain, the derivative gain was held constant at a value determined to be in the center of the operational range (300). The first set of tests was done without harvesting crop. An operational range for the P gain was set to 10-40, and four data sets were collected at P values of 10, 20, 30, and 40. The results are shown in Figure 6.2 and Table 6.1.

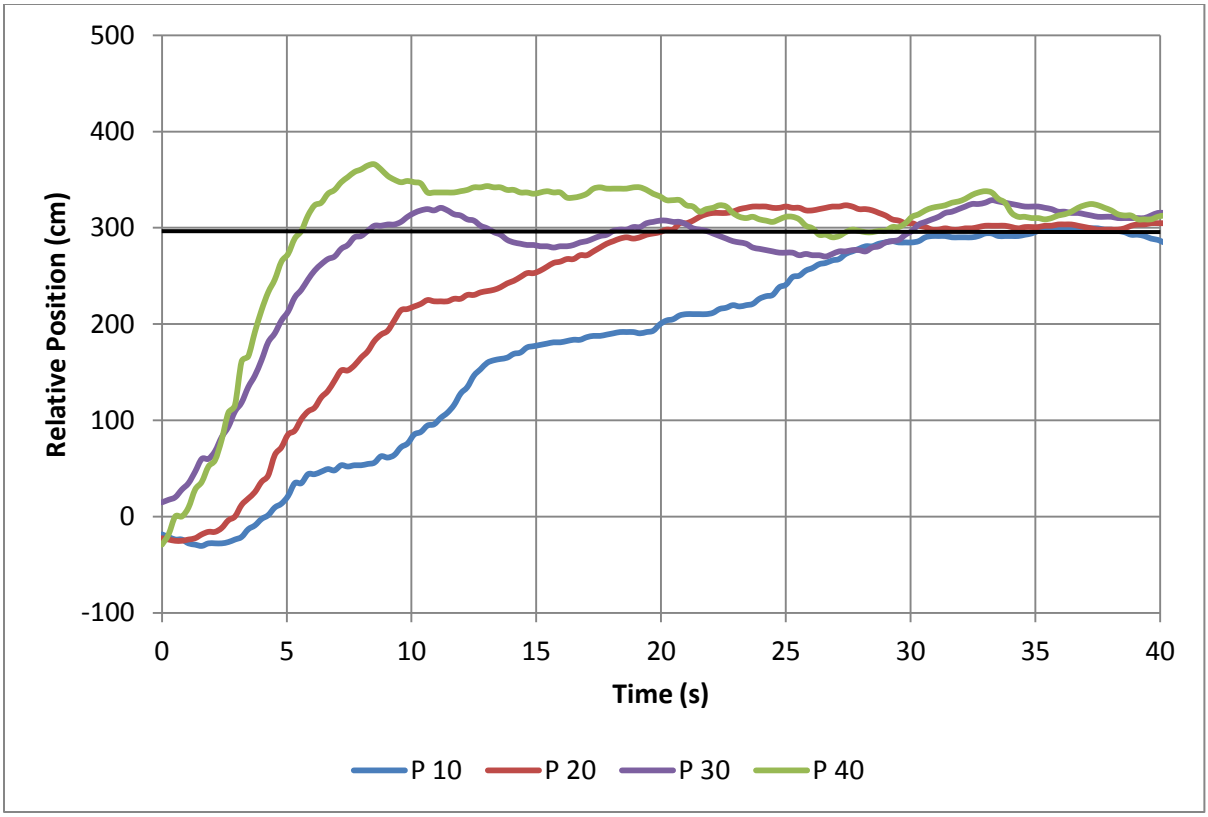

Figure 6.2: Varied P Gain with constant D Gain (300)

Table 6.1: Step Response characteristics of plot shown in Figure 6.2

P	Rise time (0%-100%) (s)	Maximum Overshoot (%)
10	35.6	-
20	20.6	6.8
30	8.3	6.7
40	5.7	19.8

The data collected at a low engine load indicated that both over damped and under damped system responses were achieved. However, the response with the lowest P gain was extremely slow, so the operational range was adjusted to a range of 15-60 for the tests completed while harvesting crop in order to achieve a broader range of response characteristics. Four data sets were collected at P values of 15, 30, 45, and 60. During these tests the derivative gain was held constant at a value of 300. The results are shown in Figure 6.3 and Table 6.2.

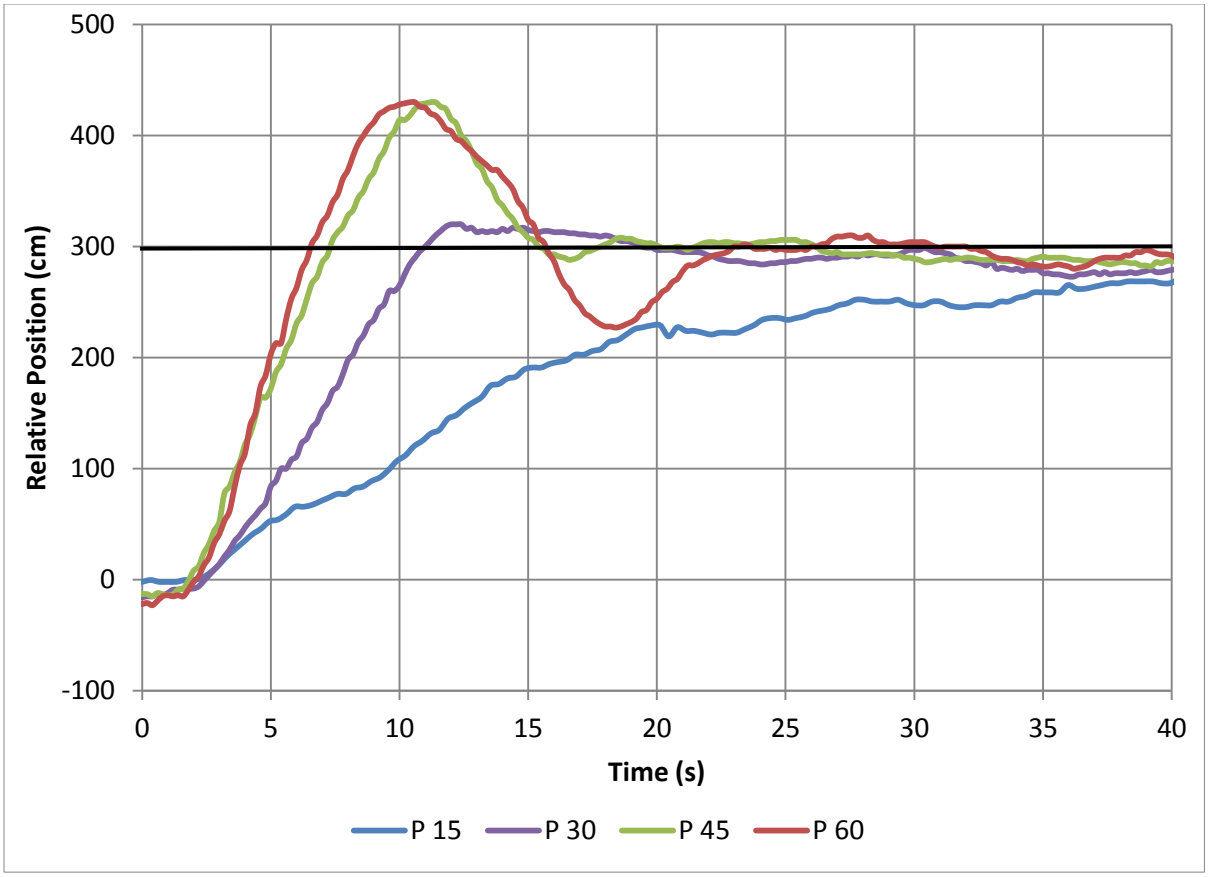

Figure 6.3: Varied P Gain with constant D Gain (300) while harvesting crop

Table 6.2: Step Response characteristics of plot shown in Figure 6.3

P	Rise time (0%-100%) (s)	Maximum Overshoot (%)
15	-	-
30	11.0	6.3
45	7.3	41.5
60	6.6	40.3

The results for both the tests done in crop and out of crop were consistent with a proportional gain value of 30 providing the most desirable response characteristics by providing a relatively quick response and small overshoot. The machine responded noticeably slower while harvesting crop and under a much higher engine load. This delayed response not only increased the rise time, but also the overshoot due to lag in machine response. In order to prevent engine overloading and slugging the machine with crop, the acceleration limiting model function was engaged for all tests completed while harvesting.

The impact of this function can be seen in the nearly identical rise characteristics for the tests completed with the P gain set to 45 and 60.

6.3.1.2. Derivative Gain Tuning

For the tests to determine the optimum derivative gain, the proportional gain was held constant at a value determined to be in the center of the operational range (30). The first set of tests was done without harvesting crop. An operational range for the D gain was set to 150-600, and four data sets were prepared to be collected at D values of 150, 300, 450, and 600. No data was collected for the D gain of 600 because the response was very over damped and the test was aborted. The results for D gains of 150, 300, and 450 are shown in Figure 6.4 and Table 6.3.

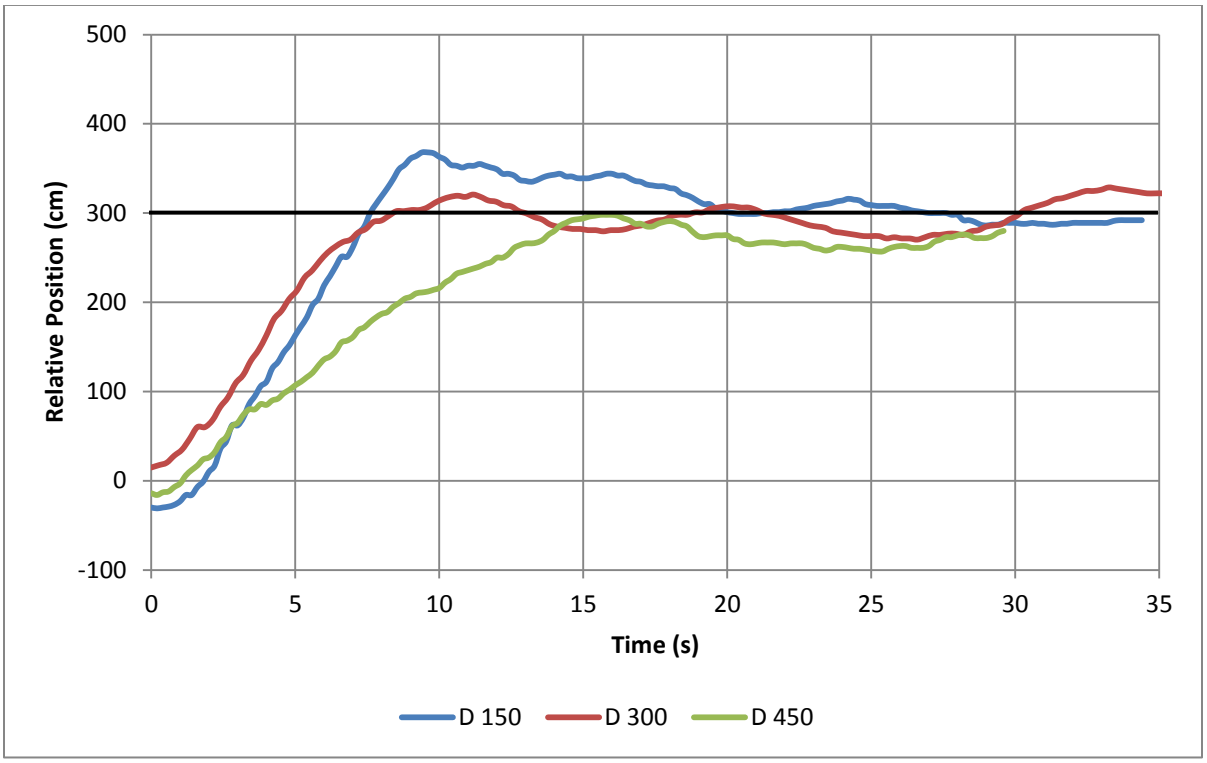

Figure 6.4: Varied D gain with constant P Gain (30)

Table 6.3: Step response characteristics of the plot shown in Figure 6.3

D	Rise time (0%-100%) (s)	Maximum Overshoot (%)
150	7.6	20.6
300	8.3	6.7
450	15.8	-

The data collected at a low engine load indicated that both over damped and under damped system responses were achieved. A second set of derivative gain tests was conducted while harvesting crop with gain values identical to the out of crop test (150, 300, 450). During these tests the proportional gain was held constant at a value of 30. The results are shown in Figure 6.5 and Table 6.4.

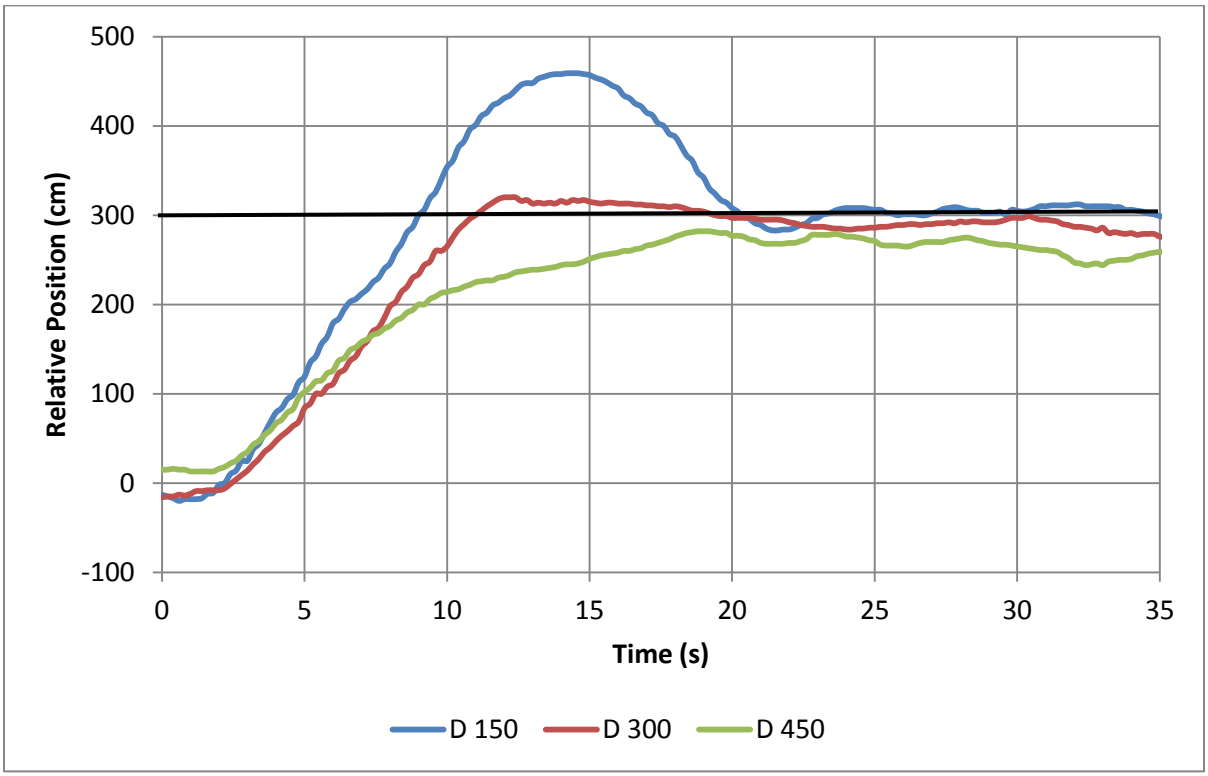

Figure 6.5: Varied D gain with constant P Gain (30) while harvesting crop

Table 6.4: Step response characteristics of the plot shown in Figure 6.5

D	Rise time (0%-100%) (s)	Maximum Overshoot (%)
150	9.0	50.7
300	11.0	6.3
450	-	-

The results for both the tests done in crop and out of crop were consistent with a derivative gain value of 300 providing the most desirable response characteristics by providing a relative quick response and small overshoot. The response for the derivative gain of 150, responded quickly, but resulted in an overshoot of 50.7%, which was much greater than the accuracy metric of 40 cm (13.33% overshoot for a 3.0 m step). The machine responded slower while harvesting crop and under a much higher engine load. This delayed response not only increased the rise time, but also the overshoot in the under damped case with the D gain set at 150. These tests provided the data necessary to confirm gain values that would be appropriate for field operation. Following this gain analysis, all field tests were conducted with a P gain of 30 and a D gain of 300.

6.3.2. Control System Response Analysis

6.3.2.1. Desired Speed and Engine Loading

Hypothesis: As the average engine load increases the rise time will also increase.

The first step in analyzing the impact of engine loading on response time was to evaluate the impact the harvest speed (control input) had on engine load. The harvest speed had a statistically significant impact on the average engine load with a P-value of 0.000, as indicated by the 95% confidence interval plot in Figure 6.6.

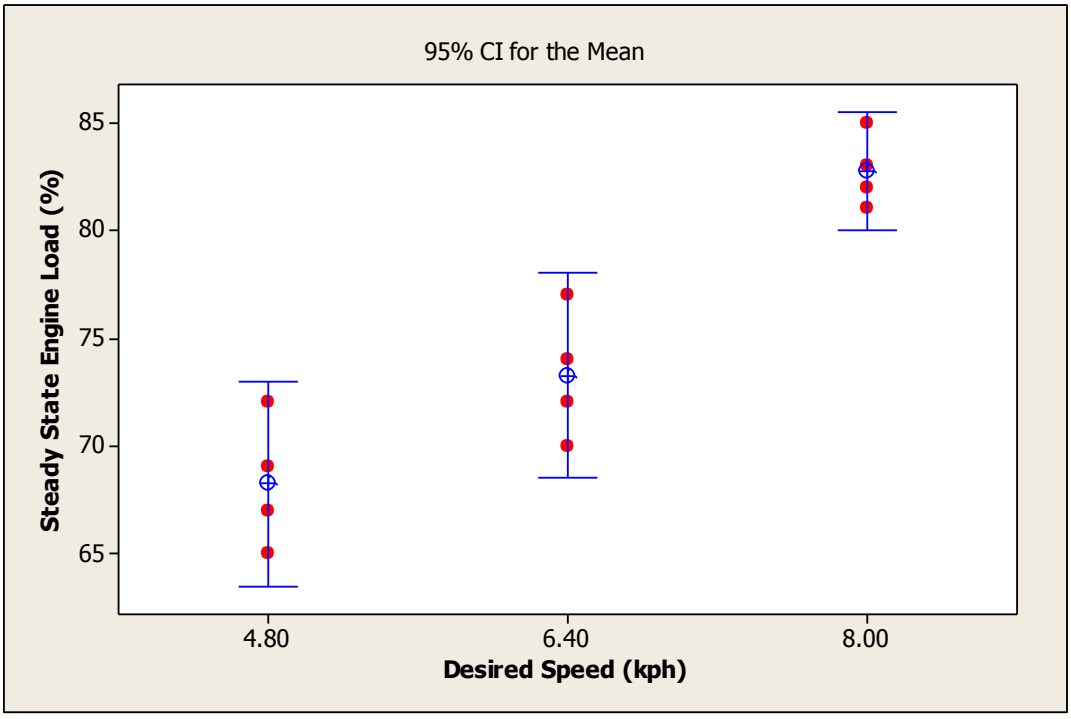

Figure 6.6: Interval plot for the steady state engine load at three harvest speeds

The varying harvest speeds were able to provide a wide range of typical harvesting engine loads (65%-85%) sufficient to conduct the analysis of engine load impact on the rise time. Four step inputs of magnitude 3m were used at each harvest speed, two in the forward direction and two in the reverse direction. Because the engine load could not be controlled precisely an interval plot was created for ranges of steady state engine load. In Figure 6.7 three engine loading ranges were used to organize the data (61%-70%, 71%-80%, and 81-90%). The impact of the engine load on rise time was found to be statistically insignificant with a P-value of 0.421. Although this was an unexpected outcome, it was a positive result for the active speed control model as it indicated repeatable and consistent performance across a wide range of typical engine loads.

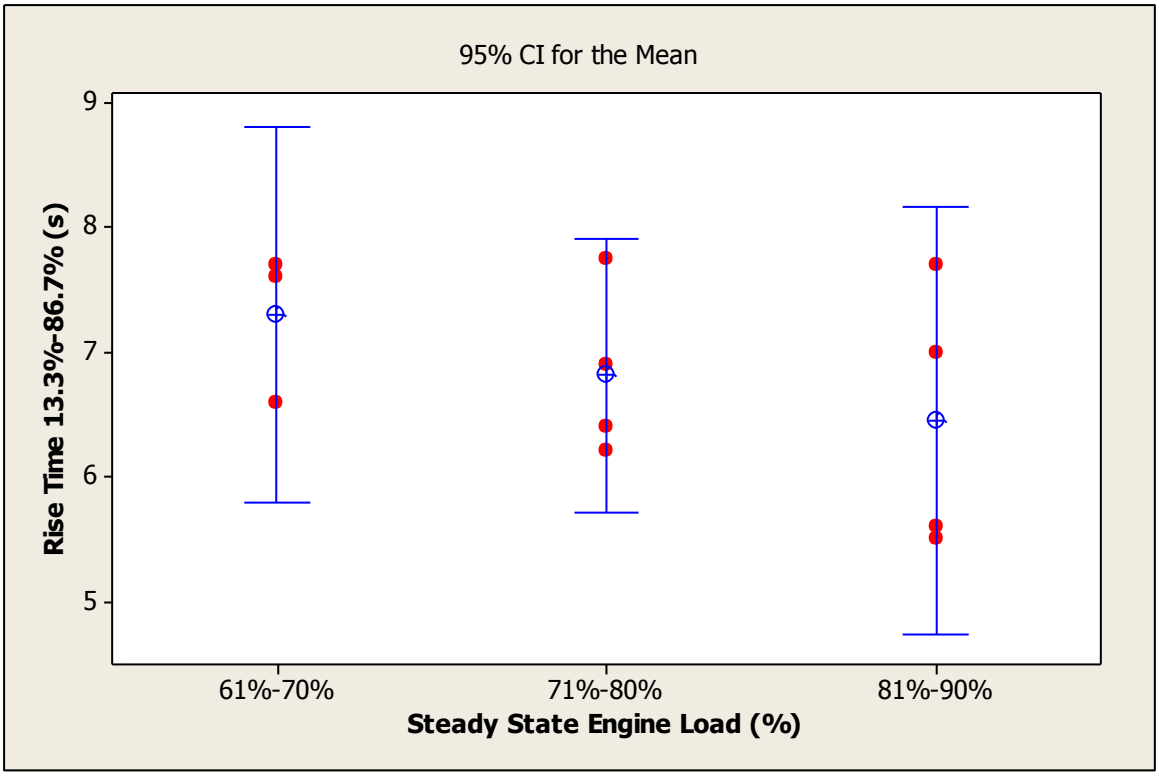

Figure 6.7: Interval plot for the rise time observed at three ranges of steady state engine load.

6.3.2.2. Saturation Model Feature

Hypothesis: As the range of the saturation model feature increases, the ΔP_{engine} *observed during a step input will also increase.*

Tests adjusting the range of the saturation model feature indicated that there was not a statistical impact on the ΔP_{engine} by the saturation ranges at a 95% confidence interval (Figure 6.8), as the hypothesis tested resulted in a P-value of 0.166. This can be partially explained by understanding that the magnitude of ΔP_{engine} was driven by the both magnitude of the acceleration and the change in velocity. Although the saturation model feature did have some control of the magnitude of the relative velocity, it did not have any control of the magnitude of the acceleration, thus limiting its ability to impactΔP_{engine}. A smaller confidence interval was observed as the saturation range increased, which was likely due to the inaccuracy of ground speed control of saturation model feature. As the size of the saturation range increases, the amount of impact and limiting it had on the control system decreases. In Figure 6.9 the response for two step inputs of -3 meters and two inputs for +3

meters highlight the difference between the largest (1.60 kph) and smallest (0.32 kph) saturation ranges. In left plot, the ground speed rarely reaches the outer bounds of the controllable range and the ground speed response is very consistent, as compared to the right plot where the minimum and maximum bounds are reached in every step response and there is greater variation in the ground speed during relative position shifts.

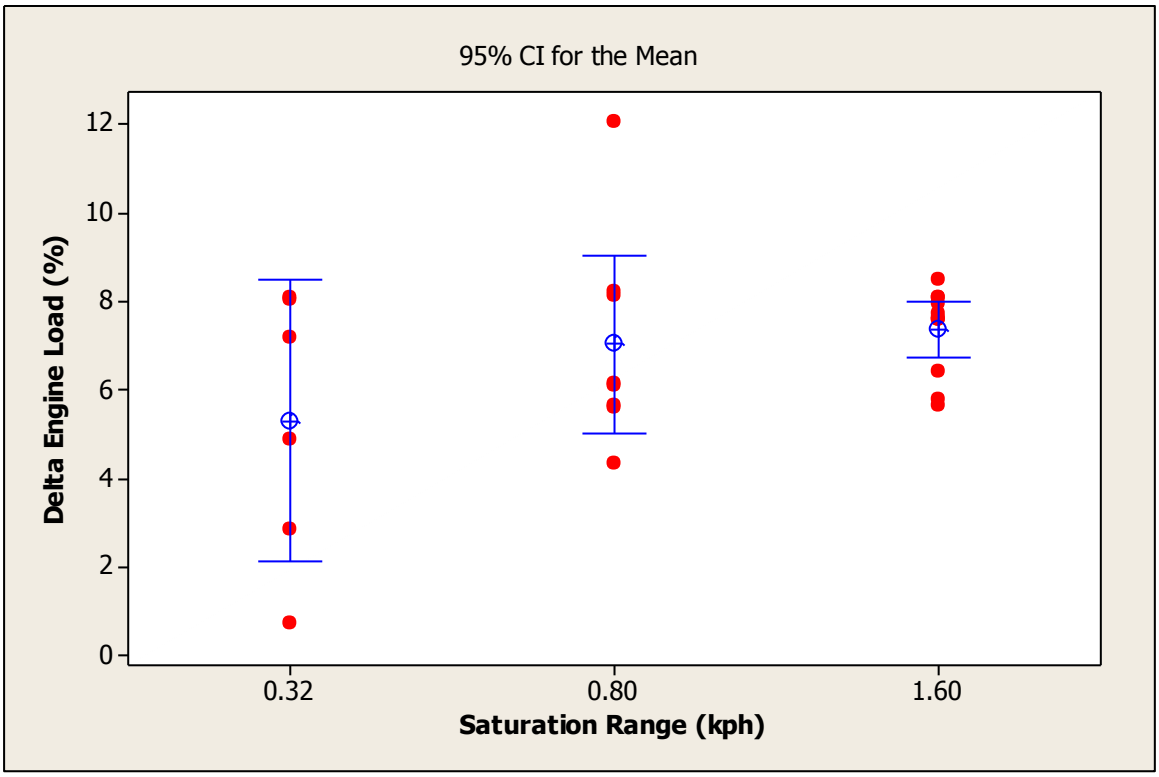

Figure 6.8: Interval plot for the ΔP_{engine} observed during step responses using three discrete saturation ranges.

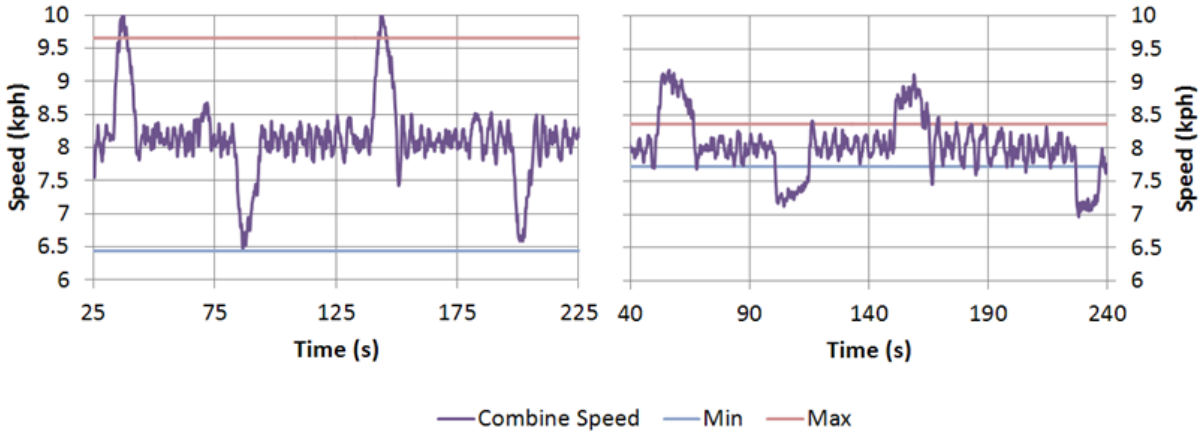

Figure 6.9: Impact of the saturation range. Range of ± 1.60 kph (left) and range of ±0.32 kph (right)

Hypothesis: As the range of saturation model feature increases, steady state error will also increase.

The steady state error was calculated by averaging the first three seconds of position data once a relative velocity of 0.0±0.1 kph was reached. With the input scheduling function enabled, the steady state error would remain constant as long as the relative position was within ±40 cm of the desired location. Control range limiting resulted in a weak statistically significant impact on steady state error by the control ranges with a P value of 0.062. A 95% confidence interval for the data is shown in Figure 6.10. The positive correlation of the data can be explained by recognizing the increased relative velocity associated with the larger control ranges. The positive linear correlation is not stronger due to inconsistency in the relative velocity with which the control model approached the desired location. This inconsistency is believed to be caused by small variations in ground speed of both the combine and the grain cart as they travel across the field as well as inconsistency in the maximum and minimum ground speed allowed by the saturation model feature.

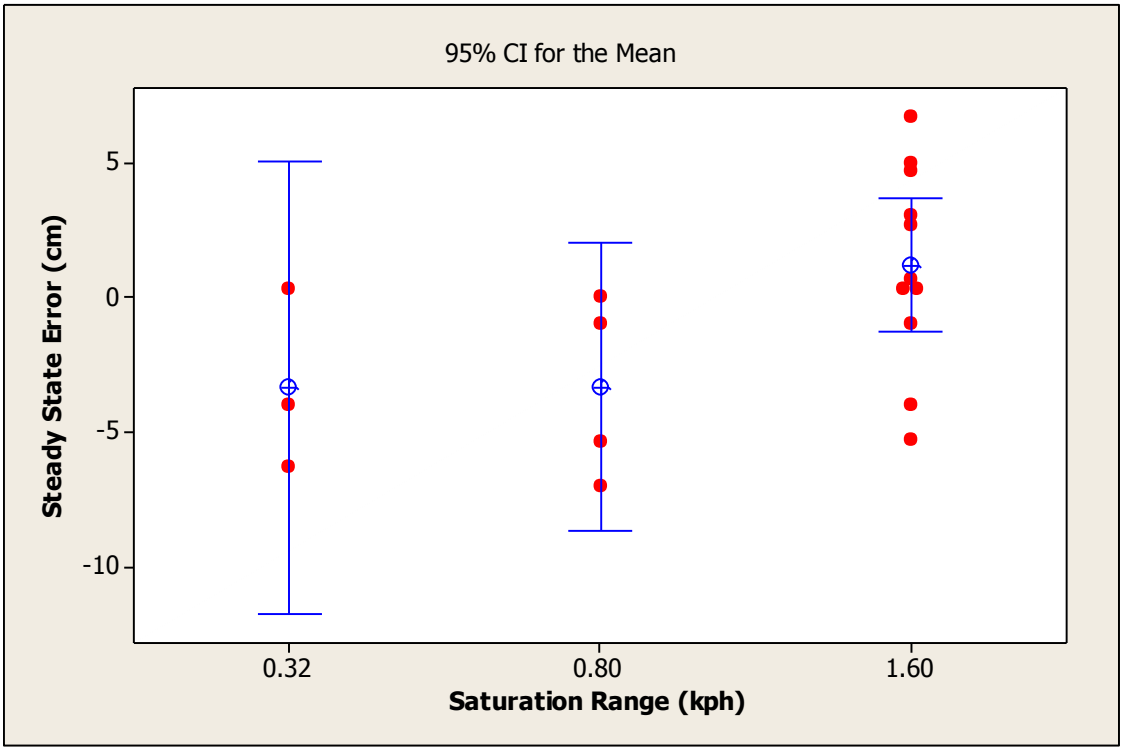

Figure 6.10: Interval plot for the steady state error observed during step responses using three discrete control ranges.

Hypothesis: As the range of the saturation model feature increases, the rise time will decrease.

Control range limiting tests indicated a statistically significant impact on rise time with a P-value 0.000. A 95% confidence interval for the data is shown in Figure 6.11, and indicated a negative correlation of the data. This response was expected because the control range limiting impacted the maximum relative velocity that could be achieved during a step response.

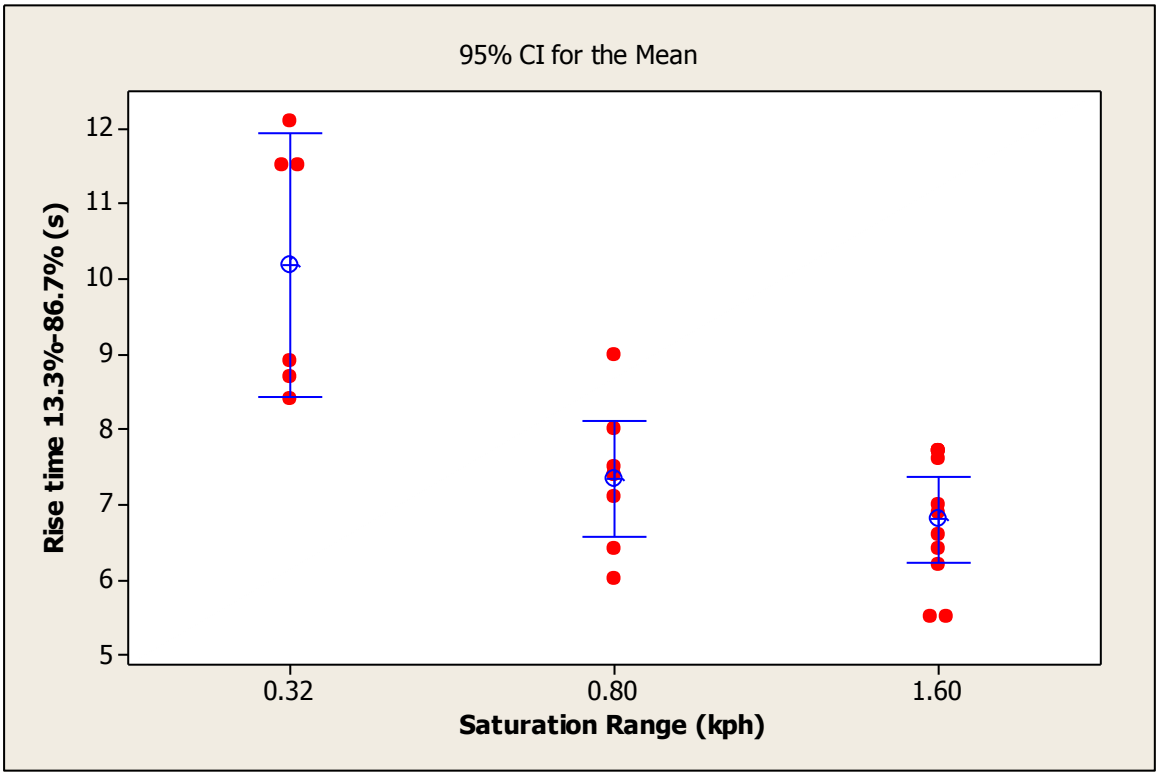

Figure 6.11: Interval plot for the rise time (13.3%-86.7%) observed during step responses using three discrete saturation ranges.

6.3.2.3. Direction of Relative Position Command

Hypothesis: The relative position shifts given in the forward direction will have a slower rise time than those given in the reverse direction.

To examine the magnitude and consistency of the ΔP_{engine}across the relative position commands the average ΔP_{engine} and standard deviation (σ) was calculated. The ΔP_{engine}, σ

was -7.185 , 1.023 for the relative position shifts of -3.00 m and 7.312 , 1.073 for the relative position shifts of 3.00 m indicating very consistent ΔP_{engine} and machine response across all the relative position commands given.

Tests of the direction of the relative position command showed a statistically significant impact on the rise time to a step input with a P-value of 0.088. This result was the opposite of the expected outcome as it was assumed that a positive change in relative velocity would take longer to achieve than a negative change in relative velocity. This result could most likely be explained by a more in depth understanding of the hydrostatic transmission on the combine. The results indicate that the transmission tended to accelerate machine faster than decelerate. Yet, with the average difference in rise time less than one second (-3.00_{avg}=7.35s, 3.00_{avg}=6.40s), overall the machine performed consistently. This data also indicated the robustness of the control model by maintaining consistent response characteristics across changing relative position commands and engine loading situations.

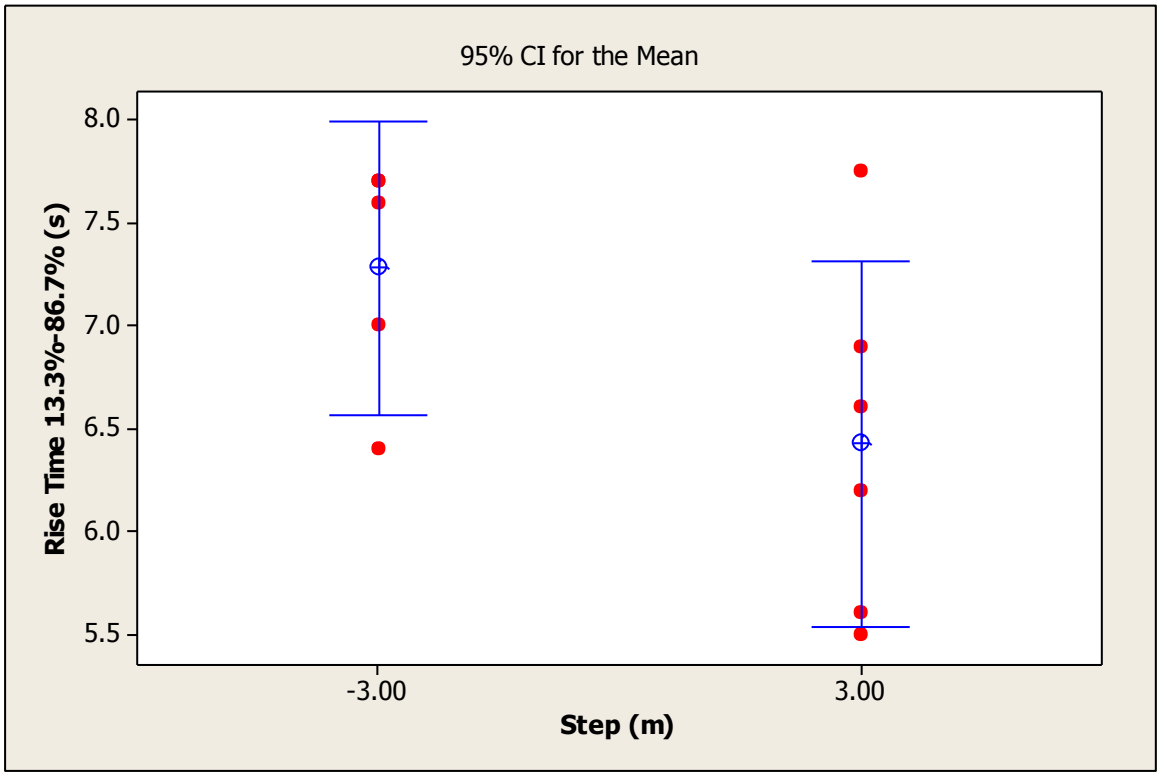

Figure 6.12: Interval plot for the rise time (13.3%-86.7%) observed during response to step inputs of +3.0m and -3.0m.

6.3.2.4. Control System Accuracy

The control system accuracy was evaluated by examining the relative position errors once a steady state was reached. In all the tests a relative position step input was given, the model would respond and reach steady state. Once steady state was reached, the test was allowed to continue for approximately 60 seconds while the combine continued to harvest crop and the grain cart traveled parallel at a near constant velocity. This data indicated the accuracy and ability of the control system to respond to normal field disturbances such as changing terrain and crop load. This procedure was conducted 12 times and resulted in a total of nearly 13 minutes of steady state data where control model controlled the speed of the combine. The average relative position error and standard deviation for each test is shown in Figure 6.13. The average relative position error varied from -23.86 cm to 28.72 cm across the 12 tests. In all of the steady state data, any relative position errors >40 cm or <-40 cm were recorded because these data points were outside the accuracy metric. The total percentage of time in which the control model operated outside of the ±40 cm metric in these 12 tests was 4.36%.

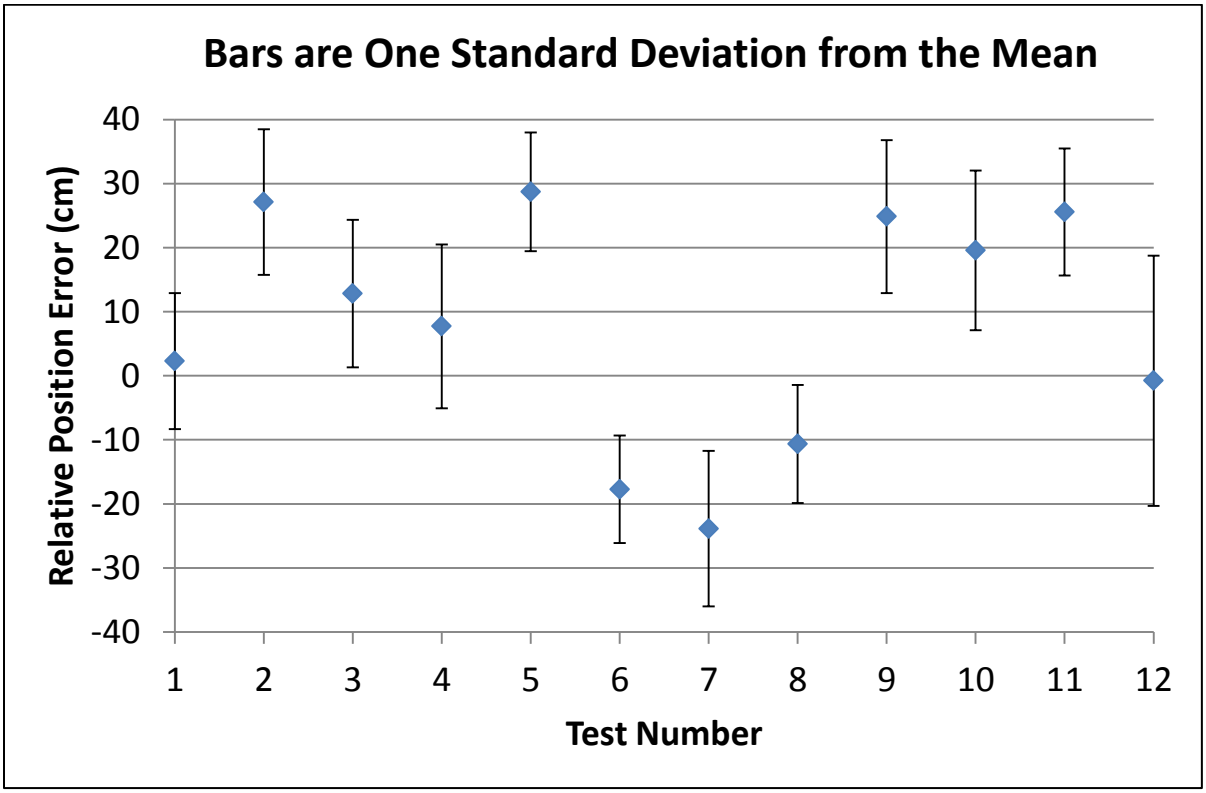

Figure 6.13: Plot of relative position error during steady state operation of relative position control model.

6.4. Conclusions

The field data and analysis presented in this chapter provided the information necessary to satisfy the three required metrics outlined in the chapter introduction, as well as the thesis objectives stated in Chapter 3.

The control system accuracy metric of ±40 cm was satisfied as shown by the data in 6.3.2.4. The control system was able to achieve a common desired relative position shift of 3 m without overshooting or undershooting the desired location by more than 40cm. Once the control system reached steady state, it was very successful in keeping the relative position error less than 40 cm by only allowing a position error > 40 cm or <-40 cm 4.36% of the time.

The ΔP_{engine} <10% metric was satisfied in 17 out of the 18 test cases as shown by the data presented in 6.3.2.2, with the one exception exceeding the metric by only 2% ΔP_{engine} . Based on these results, it was determined that the acceleration limiting model function designed to limit differential engine load was a success. Keeping in mind that ΔP_{engine} <10% metric was set in order to guide model design and development, not as an inflexible model requirement, it was determined that meeting the metric nearly 95% of time was sufficient.

The response time metric of achieving a relative position shift of 3 m in 10 seconds was achieved in two of the three tests cases as shown in 6.3.2.2. The ranges used for the saturation model function had a statistically significant impact on the rise time, and due to the metric definition it would be recommended to avoid using a saturation range of ±0.32 kph due to the slow response.

The three objectives outlined in Chapter 3 were all successfully completed. The success of objective 1 was clear in the preliminary testing as well as the final field testing. In all tests, the control method of altering the analog voltage to the machine control proved to a safe a reliable means of speed control. The control model development completed in Chapter 5 successfully generated a control model architecture that proved to be a successful control design for relative position control. The control model was designed to allow for model features to be added addressing specific control issues as they surfaced. The final result was a control system that had the necessary

features in place to meet all three of the design metrics, which successfully completed objective 2. Field tests were conducted in multiple field locations and on multiple days in order to observe system performance across a normal set of field conditions. In all of the tests cases, the system performed well, allowing for active combine speed control to successfully control the relative position to a grain cart within the specified design metrics, thus accomplishing objective 3. With all three project objectives successfully completed, the design and development work of this project was concluded.

With the completion of the project, several additional steps were identified as possible future work. It is believed that the gain scheduling could still improve performance, but refinement of the feature is needed. A possible first step would be to reduce the gain of D at a linear rate as the position error decreases, as opposed to the current method which eliminates the D gain once reaching the gain scheduling threshold. Also, a similar development is recommended for the input scheduling model feature. In examining Figure 6.13 it clear to see that once a position error less than 40 cm is reached, the relative position error changes very little. In order to improve upon this even more, it is suggested that the input scheduling model feature also use a composite of both position and velocity error inputs to determine control signal, which would likely reduce the average error observed when relative position errors are ±40 cm of the desired location. Additional work is also needed to improve the saturation model feature. Although the model feature did accomplish the goal to avoid large speed changes, it lacked precise control of ground speed to match the user inputs of minimum and maximum speed. It is believed that this feature could be improved by using the ground speed and acceleration to predict when the combine will reach a minimum or maximum speed. This prediction would allow the feature to avoid the large ground speed overshoot observed using the current design.

With the review of model performance and results upon the project completion, an ideal system operating configuration can be recommended. In this configuration, it would be recommended to use inputs of both relative position and velocity as both of these inputs were required in order to achieve optimum response. The acceleration limiting model feature should be implemented in the same form in which it was designed and

used in this project. The input scheduling and saturation model features, could be used in their current form, but the recommendations suggested earlier should be implemented to further improve performance. The gain scheduling model would need to have the suggested changes made before using this feature, as the model feature as designed had a significant negative impact of system performance.

Overall, the project was a success. The active combine speed control system allowed for accurate relative positioning of a grain cart across typical field conditions, an innovative accomplishment not seen to date by any combine manufacturer.

References

Auckland, Robin A., Oliver M. J. Carsten, Martin C. Levesley, David A. Corolla, and Warren J. Manning. "Dynamic Performance of Adaptive Cruise Control Vehicles." *SAE 2005 World Congress & Exhibition.* Warrendale: SAE, 2005. 1-6.

Bauer, Horst. *ACC Adaptive Cruise Control.* Germany: Robert Bosch GmbH, 2003.

Bengea, Sorin C., Peter B. Eyabi, Michael P. Nowak, Richard M. Avery, and Robert O. Anderson. "Adaptive Cruise Control for Heavy-Duty Vehicles: A Torque-Based Approach." *SAE 2006 World Congress & Exhibition.* Warrendale: SAE, 2006. 1-6.

Brent Equipment. *Avalanche Grain Carts.* 2012. http://www.brentequip.com/graincarts/avalanche/ (accessed 1 26, 2012).

Caterpillar. *Autonomous Mining.* November 28, 2011. http://catminestarsystem.com/articles/autonomous-mining-improving-safety-and-increasing-productivity.

CNH North America. *Case IH Wins Gold and Silver Medals at SIMA Innovation Awards.* December 6, 2010. http://investors.cnh.com/phoenix.zhtml?c=61651&p=irol-newsArticle&ID=1504751&highlight=.

Deere & Company. *John Deere Introduces New Machine Sync Technology to Optimize Harvesting in the Field.* August 25, 2011. http://www.deere.com/wps/dcom/en_US/corporate/our_company/news_and_media/press_releases/2011/agriculture/2011aug25_machinesync.page.

Elfes, Lee E. United States Patent 3,563,013. 1971.

Engineering and Mining Journal. *Cat Launches New MineStar System with Expanded Features and Capabilities.* August 11, 2011. http://www.e-mj.com/index.php/departments/operating-stratagies/1131-cat-launches-new-minestar-system-with-expanded-features-and-capabilities.html.

Fardal, Randolph G., and Calvin P. Rickerd. United States of America Patent 4130980. 1978.

Herbsthofer, Franz Joseph. United States Patent 3,609,947. 1971.

John Deere. "New John Deere 70 Series Combines." Lenexa, 2007.

Kingma, H. "Thresholds for perception of direction of linear acceleration as a possible evaluation of the otolith function." (BioMed Central - Ear, Nose & Throat Disorders) 5, no. 5 (2005).

Komatsu. *Autonomous Haulage System - Komatsu's Pioneering Technology Deployed at Rio Tinto Mine in Austrailia.* November 28, 2011. http://www.komatsu.com/ce/currenttopics/v09212/index.html.

New Holland . *CR Twin Rotor Combines.* 12 1, 2011. http://agriculture.newholland.com/us/en/Products/Harvesting-Equipment/CR9000/Pages/Feeding_details.aspx.

Onken, Reiner, and Axel Schulte. *System-Ergonomic Design of Cognitive Automation.* Berlin: Springer-Verlag, 2010.

Pueboobpaphan, Rattaphol, and Bart van Arem. "Driver and Vehicle Characteristics and Platoon and Traffic Flow Stability." *Intelligent Transportation Systems and Vehicle-Highway Automation*, 2010: 89-97.

Stone, M.L., R.K. Benneweis, and J. Van Bergeijk. "Evolution of Electronics for Mobile Agricultural Equipment." *Transactions of the ASABE*, 2008: 385-390.

Taylor, Randal K., Mitch Hobby, and Mark D. Schrock. "Evaluation of an Automatic Feedrate Control System for a Grain Combine." *ASAE Annual International Meeting.* Tampa: ASAE, 2005. 1-12.

Vollrath, Mark, Susane Schleicher, and Christhard Gelau. "The influence of Cruise Control and Adaptive Cruise Control on driving behaviour – A driving simulator study." *Accident Analysis and Prevention*, 2011: 1134-1139.